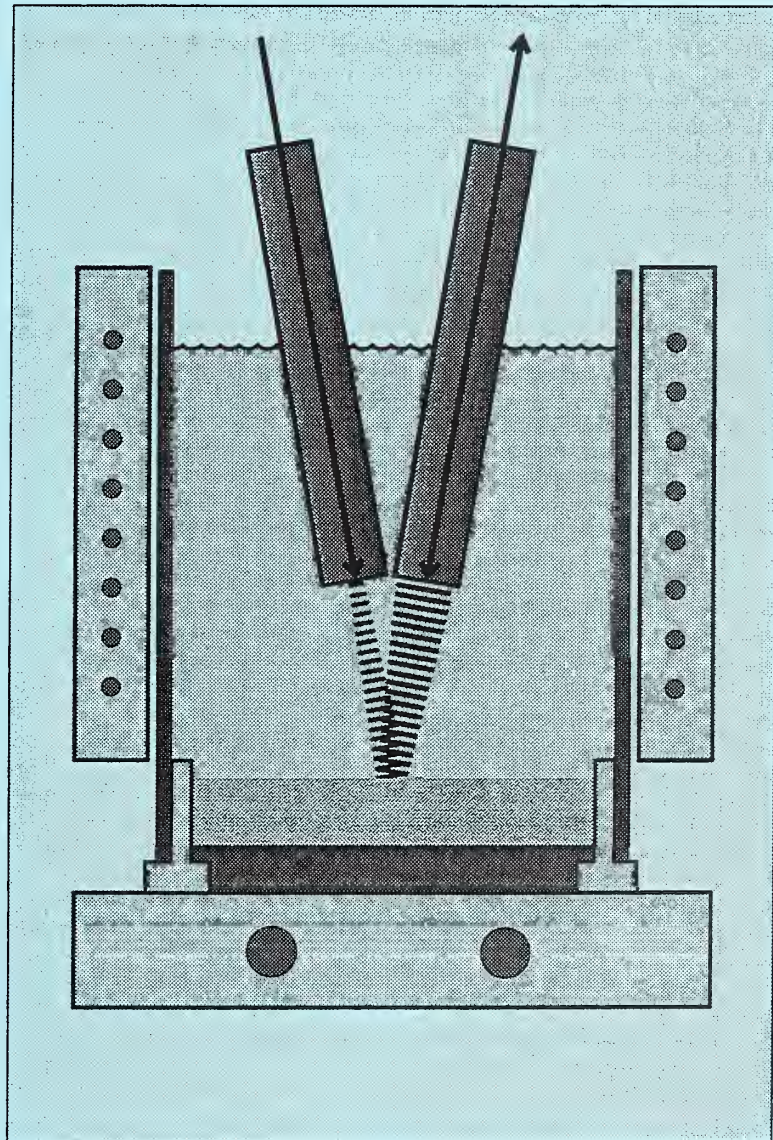MSEL

Materials Science and Engineering Laboratory

INTELLIGENT PROCESSING OF MATERIALS

NAS-NRC
Assessment Panel
February 2-3, 1993

NISTIR 4963
U.S. Department of Commerce
Technology Administration
National Institute of Standards
and Technology

Technical Activities 1992

Apparatus used in the development of an ultrasonic sensor for characterizing liquid/sold interfaces in directionally solidifying metals. A crucible containing liquid tin is cooled at its base such that the tin solidifies upwards. Ultrasonic waves are generated directly in the liquid by a pulsed Nd-YAG laser beam which passes through an immersed silica rod. A beam from a He-Ne laser interferometer passes through a second immersed rod and detects waves which are reflected off the interface.

MSEL

Materials Science and Engineering Laboratory

INTELLIGENT PROCESSING OF MATERIALS

H.T. Yolken, Chief
G. Birnbaum, Senior Scientist

Technical Activities 1992

Certain companies and commerical products are mentioned in this report. They are used to either completely specify a procedure or describe an interaction with NIST. Such a mention is not meant as an endorsement by NIST or represent the best choice for that purpose.

TABLE OF CONTENTS

NDE SENSORS, METHODS, AND STANDARDS

APPENDICES

INTRODUCTION

In 1992, the Office of Intelligent Processing of Materials continued its major focus on cooperative programs with industry to establish concepts for intelligent processing of materials. The research activities are grouped into two major areas: Materials Processing; and On-Line and Nondestructive Evaluation (NDE) Sensors. The first deals with process modeling, development of sensors for on-line process control and the development and validation of process models, and in some cases, integration of these elements with an expert computer control system to demonstrate key aspects of intelligent processing of materials. Whereas, in the first area the research on sensors is tied closely to specific processes, the work on NDE sensors in the second area, while motivated by on-line applications, is not necessarily linked with process models or intelligent processing per se. Also included here is an effort in the calibration and standardization of NDE sensors for post manufacturing inspection. This overall approach provides enhanced opportunity to link research in this program with other NIST efforts in materials science and engineering, and provides for enhanced interactions with industry.

This year researchers involved in the Intelligent Processing of Materials program made a number of significant scientific and technical advances. This report contains descriptions of these technical advances, and several of the noteworthy advances are highlighted below along with some plans for future research.

Materials Processing

o   NIST researchers collaborating with U.S. industry in the NIST Consortium on Intelligent Processing of Rapidly Solidified Metal Powders by High Pressure Gas Atomization have successfully transferred consortium developed particle size sensor methodology to consortium members. This methodology is crucial for on-line process control and was transferred utilizing a workshop and written reports.

o   Planning was completed with the American Iron and Steel Institute for a major research program on steel processing. The two NIST proposals involve developing process models for the thermomechanical processing of steel and developing magnetic sensors for on-line determination of the mechanical properties of steel sheet. These proposals have been approved by AISI and DOE for funding starting in 1993. Preliminary research on these two projects has resulted in significant progress. A process model was developed for the thermomechanical processing of Nb-treated microalloyed steel to be used in automotive applications. In addition, the validity of the on-line magnetic sensor was firmly established through research that showed a close correlation of the magnetic properties determined by the sensor with the yield strength.

o   Intelligent processing strategies for gas metal arc welding require a knowledge base relating molten metal droplet detachment from the welding rod (electrode) to the workpiece. To meet this need, NIST and MIT researchers have developed a process model of the melting electrode during welding and have successfully validated the model with experiments.

o   Planning was completed for a NIST/U.S. industry consortium on the processing of polymer blends. The objective of the consortium is to understand and control the processing and kinetics of mixing/demixing. Mixing/demixing is critical in all polymer blends/alloys processing designed to control microstructure and morphology of the final material and its tailored properties.

Research was expanded this year into two additional areas to support the planned consortium start-up early in 1993. This research includes understanding the shear mixing/demixing and phase separation kinetics after cessation of shear, and interfacial modification and control.

o Planning was completed for a consortium on casting of aerospace alloys. This consortium aims to improve casting quality by utilizing intelligent processing concepts involving process modeling, process sensing, thermophysical properties data, rapid prototyping, model validation and systems integration. This will be a distributed research effort with aerospace companies, universities, non-profit laboratories and federal agencies. The planning was a cooperative undertaking by the Aerospace Industries Association, aerospace companies, universities, non-profit labs, NIST, and other federal labs. The consortium is expected to get started early in 1993 with NIST in-house research carried out in the Metallurgy and Materials Reliability Divisions.

o Planning was completed for a consortium on improving paint finish. This effort will include research on determining and controlling paint finish quality on automobiles and other sheet metal products. The Building Materials Division has taken the lead in planning this effort jointly with the Intelligent Processing of Materials program with the research to be carried out jointly by several NIST divisions. We are hopeful that this consortium will attract enough industrial members to be established in the first quarter of 1993.

On-Line and NDE Sensors

o Eddy current methods provide a rapid means of performing non-contact measurement of resistivity of metals during processing. If the effects of composition can be accounted for, then the resistivity measurements may be used to obtain an on-line determination of the temperature. A simulation test at an aluminum plant to study an eddy current method for monitoring temperature during hot-rolling of aluminum sheet showed that the correction for composition is feasible.

o Colloidal processing of powders for advanced structural ceramics requires stringent control of particle dispersion in liquids. To this end, work was focussed on electrokinetic sonic amplitude (ESA) measurements in silicon nitride powder suspensions in water. Such measurements were made to study the performance of acidimetric-alkalimetric titrations and the determination of the powders' isoelectric point (the pH at which the particles are electrically neutral). A critical study was also completed which showed a linear relation between surface oxide layer thickness and isoelectric point of silicon nitride suspensions, irrespective of particle size.

o In a ceramic green body, the binder distribution is a critical parameter that affects the final ceramics's properties and reliability. The binder distribution in green bodies consisting of silicon nitride powders with either polyethylene glycol or polyvinyl alcohol binders was studied with an NMR imaging system based on using a large magnetic field gradient.

o Users of laminography systems (a type of radioscopy that can focus on a single plane) for circuit board inspection identified a need for several calibration devices. One of these was satisfied by developing a calibration board for the X-Y stages of automated radioscopy systems. The board is designed to directly measure the positioning accuracy and geometrical magnification of the system.

o   Laser-ultrasonic techniques for performing ultrasonic measurements on steel alloys at elevated temperatures but below the melting point were investigated. Many processes for hot shaping of alloys require that the bulk temperature exceed a threshold value before processing can begin. Studies were made which show that ultrasonic wave velocities correlate closely (almost linearly) with temperature in the range 20 to 1000 °C for AISI 303 and 304 steel.

In closing, I would like to repeat what I have said in past years. The prospects look bright for our program on intelligent processing of materials. This Office is positioned to have a major impact on American industry through its research programs, active communication with a broad range of materials processing specialists, and a growing collaboration with industry to transfer elements of intelligent processing to the American factory. Technology transfer will continue to gain importance in research planning and execution. We look forward with great enthusiasm to working with the American Iron and Steel Institute and their member companies, producers of advanced metal alloy, the polymers industry, the ceramics industry, and other users and producers of advanced materials. For more information on projects in this report, kindly contact the individual investigators, or contact the Office of Intelligent Processing of Materials, Materials Building, Room B342, National Institute of Standards and Technology, Gaithersburg, Maryland 20899 (301-975-5727).

H. Thomas Yolken, Chief
Office of Intelligent Processing of
Materials

Intelligent Processing of Rapidly Solidified Metal Powders by Inert Gas Atomization

S. D. Ridder (301-975-6175) and F. S. Biancaniello
Metallurgy Division, Materials Science and Engineering Laboratory

G. E. Mattingly (301-975-5939) and P. I. Espina
Process Measurements Division, Chemical Science and Technology Laboratory

T. Vorburger (301-975-3493)
Precision Engineering Division, Manufacturing Engineering Laboratory

T. Hopp (301-975-3545) and S. A. Osella
Factory Automation Systems Division, Manufacturing Engineering Laboratory

This report, although summarizing fiscal year 1992 activities, in reality represents the results of an ongoing research program which began more than seven years ago when metal powder was first produced in the NIST-Metallurgy Division's SiGMA system (Supersonic inert Gas Metal Atomizer). More explicitly, it builds on the previous three year NIST/US industry consortium research program on this process which ended in July of 1990. This Phase 2 consortium (outlined in the 1991 IPM annual report) continues with a focus on process modeling, real-time particle size sensing, and on-line control. The consortium was initiated using cooperative research and development agreements, direct contracts, and/or work requests with Ampal/Metallurg, Crucible Materials Corporation, DOE - Office of Industrial Processes, General Electric Aircraft Engines, Martin Marietta Energy Systems, Inc., and United Technologies - Pratt & Whitney. The overall research goal of the consortium is to successfully utilize intelligent processing of materials (IPM) concepts and systems to atomize Inconel alloy 625. An IPM system is composed of an expert computer controller, on-line sensors, process models and associated materials properties data. The accomplishment of the consortium goal will result in several subsystems and methodologies that are made available to consortium members as they reach a usable and/or functional stage of development. Examples of currently available technologies are the Expert Control System Shell (ECSS) code that runs on Macintosh computers, the particle sizing code written in C and the Computational Fluid Dynamics (CFD) code written in Fortran so as to be portable to most computer systems. These and other technologies have evolved as needed to meet project objectives (updates are continuously available).

At the last consortium annual meeting (March 17, 1992), the use of workshops was proposed as another method of transferring these technologies to the consortium members. The first of these single-purpose tutorials for consortium members was held July 14th and 15th, 1992 at NIST. It covered metal powder safety topics and it described and discussed the use of off-line and in-situ particle sizing hardware and software. Subsequent workshops will be planned to cover other subject matter, in particular the use of expert system based controllers, and CFD models for the gas and the liquid flows.

(1) Process and Model--Guided by CFD results to date several changes have been made to the atomization system to enhance process control and to aid the process modelling efforts. The inert gas back-fill and melt chamber/atomizing chamber differential pressure supply plumbing now includes a gas flow rate sensor and control system that allows the ECSS to control this differential pressure. This added gas flow rate sensor combined with a similar device in the atomizing gas supply will provide needed data for the processing model. A new exhaust system has been completed that incorporates a two-fold increase in capacity as well as ECSS control of the through-put.
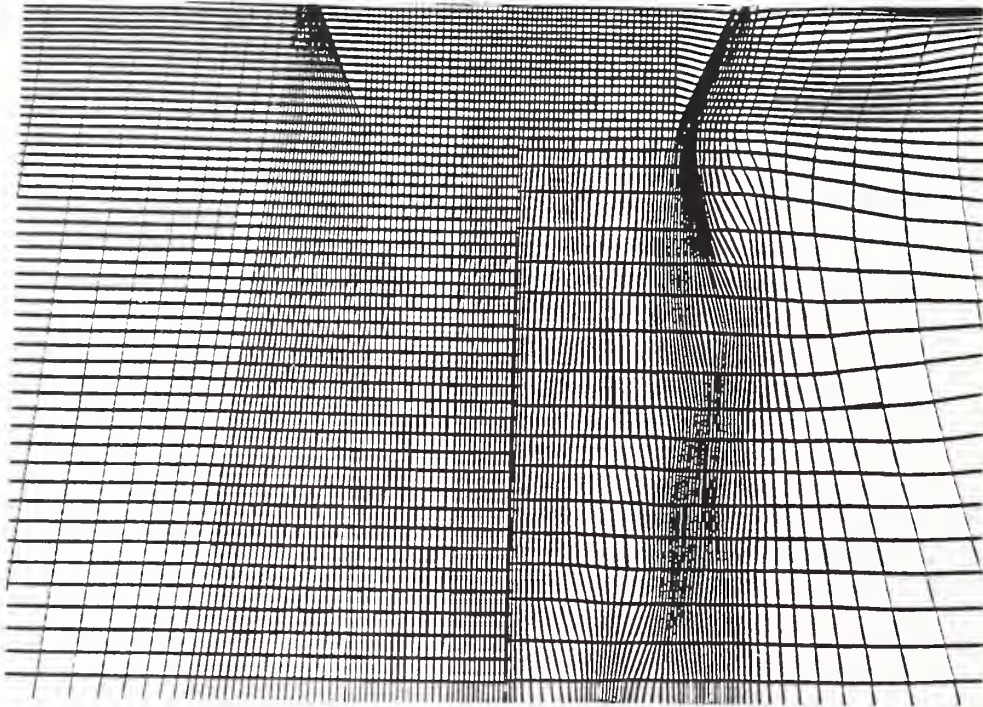
Fig. 1. Detail of a portion of a CFD grid before and after adaption (left and right respectively). The grid spacings after adaption are optimized to better resolve gradients in the gas only flow.

The CFD code for gas-only flow modeling has been modified to include adaptive grid generation. This feature more accurately locates shock waves and high shear regions by repositioning the calculation grid points as the solution relaxes. The previous technique required a long and tedious trial and error method of grid generation for each geometry and jet exit pressure studied, and the results were not as accurate since optimum grid spacings were never achieved. Figure 1 shows a portion of a CFD grid before and after adaptation using this new CFD code. A paper will be presented that covers this topic in detail at the ASM-TMS fall 1992 meeting in Chicago.

(2) Particle Size Sensor--A persistent problem which hindered the acquisition of particle size distribution data via Fraunhofer diffraction was laser beam "steering". Although it is difficult to ascertain all contributing sources to this phenomenon, it is believed that the principle malefactor is a series of refractions the laser beam undergoes as it passes through the view-ports used for on-line particle sizing. In particular, the window cleaning gas jets produce a severe temperature gradient that defocuses the laser beam and shifts undiffracted light onto inner detector elements of the photo-diode array. The result is a distortion of the diffracted light intensity distribution used to determine particle size. Recently the addition of gas heating (to reduce the temperature gradient with a corresponding reduction in the signal distortion) and software modifications have significantly reduced this problem.

Current activities in sensor improvement have focused on instrument calibration. The detector array used to collect the light intensity distribution data consists of 31 individual, solid-state detector elements produced by photo-etching on a silicon semi-conductor substrate. The sensitivity of each detector element is a function of the deposit's actual area and conversion efficiency, neither of which is identical on any two of these arrays. To determine the individual gain factor for each detector element

identical on any two of these arrays. To determine the individual gain factor for each detector element the array must be illuminated with a well defined light source while measuring the light intensity distribution. A gain factor is then assigned to each of the array elements and used to adjust the measured intensity values. The instrument manufacturer provided a calibration file consisting of the necessary 31 gain values, however, recent work with well characterized diffraction sources suggests that these values are not correct. Calibration experiments are now under way that will verify or correct these values and establish procedures for calibrating other Fraunhofer diffraction instruments.

(3) Expert Control System Shell (ECSS)--The ECSS was improved and expanded to incorporate new features which were required to extend the scope of the experimentation on SiGMA. Firstly, the memory management was made more efficient by making use of the MacIntosh resource and memory manager capabilities. This feature was critical due to the heavy use of memory by the ECSS. Next, more powerful knowledge-base construction capabilities were added to the ECSS. In particular, constants and global variables are now allowed which improve both the efficiency of the ECSS as well as its ease of use. A number of intrinsic functions, such as math, file I/O, and string manipulation functions, were added to the knowledge-base function library. Additional actuators and displays are available now. Specifically, the histogram display permits the presentation of particle size and light intensity distributions acquired from the particle sizer. The data management and play back utilities have been expanded and made more user-friendly. The ECSS allows the conversion of run data to spread-sheet formats. It also allows the operator to review run data in play back mode either in real-time, fast-forward, or frame-by-frame. Possibly the single most important improvement is the capability to include device drivers and knowledge-base functions directly into a controller file. This feature permits quick inclusion into a controller of new data acquisition systems and arbitrarily complex control functions.

The SiGMA controller was modified to incorporate improvements to the atomization run start, stop, and restart capabilities. In particular, the run start and restart sequencings were streamlined so that they would be as similar as possible. The only difference between the two sequences now is that in the restart sequence the stopper rod is not lifted. The restart capability is required in the event that the stopper rod fails to lift automatically necessitating the stopper rod to be lifted manually. The atomization run stop sequence was modified to alleviate some of the problems associated with particles collecting on the diffraction instrument view-port windows. The stop sequence now waits 2.5 seconds after the atomizing gas has been turned off to shut down the vacuum cleaners. This procedure allows the remaining powder left in the atomization chamber and exhaust tube to be vacuumed out. Previously, the remaining powder would recirculate, leaving the powder particles to accumulate on the windows, which prevented a post-run measurement of the diffraction instrument "background" level.

PUBLICATION

1.   S. D. Ridder, S. A. Osella, P. I. Espina and F. S. Biancaniello, "Intelligent Control of Particle Size Distribution During Gas Atomization," Inter. J. of Powder Metall., 28, 2 (1992).

Steel Sheet Texture and Formability

A. V. Clark (303-497-3159), S. R. Schaps, C. M. Fortunko, and M. L. Renken
Materials Reliability Division, Materials Science and Engineering Laboratory

M. G. Lozev, Guest Researcher; on leave from Technical University of Plovdiv, Bulgaria

Steel sheet finds wide use in many industrial applications. Common examples are appliances and containers. An application of particular importance is production of automobile body parts; here, sheets are formed to produce a variety of shapes such as hoods, door panels, etc. An important parameter in this application is the r-value, or plastic strain ratio. This is defined as: $r = \epsilon_w/\epsilon_t$, where ϵ_w and ϵ_t are width and thickness strain which result when subjecting a tensile specimen to plastic deformation. Higher r-value implies less thinning of the sheet during forming. The texture (preferred orientation of grains) in the sheet causes the r-value to be anisotropic in the plane of the sheet.

It now appears possible to perform on-line characterization of r-value. An approach being pursued in the U.S., Europe, and Japan is the use of noncontacting ultrasonic transducers called EMATs (electromagnetic-acoustic transducers). EMATs use the following (simplified) transduction mechanism. A current is driven through a coil at rf frequencies; this generates an image eddy current $\underline{J}$ in the surface of the nearby specimen. The current is reacted with a static magnetic induction, $\underline{B}$; this gives a dynamic force $\underline{J} \times \underline{B}$ which sets up a vibration of the ions in the metal. This acts as a localized forcing function for excitation of elastic waves.

The American Iron and Steel Institute has specified a goal of resolving the average r-value $\bar{r}$ to an uncertainty of ± 0.05 on sheet moving at about 3 m/s; this is typical of speeds in a continuous annealing line. To try to obtain this goal two different sensor configurations have been studied. One involves the propagation and reception of waves guided in the plane of the sheet. Typically, waves are propagated at angles of 0°, 45°, and 90° to sheet rolling direction. The second approach uses longitudinal and shear waves propagating through the thickness of the sheet. An array of EMATs for guided wave propagation has been constructed and tested on steel sheet moving at 3 m/s. A device to move specimens at this velocity has been constructed jointly by NIST and researchers at Ford Motor Company; this is illustrated in Fig. 1.

Error analysis revealed that to achieve the AISI-specified r-value resolution requires that velocities of guided waves be accurately determined to $\pm 0.2\%$ on moving sheet. A theoretical and experimental study was done to characterize artifacts which could degrade velocity measurement resolution [1-3]. Results of the study were used in optimizing the EMAT array and its associated electronics. Experiments performed on the moving sheet device indicated that, after optimization, the EMAT array had the necessary velocity resolution for on-line application [2-3]. The advantage of the guided-wave EMAT array is its ability to determine r-value in different directions (recall that r is anisotropic). The disadvantage is that it requires multiple transducers and fixturing to hold the sheet flat. The alternative approach, using longitudinal and shear waves propagating in the sheet thickness, can overcome these limitations (however, it can only determine the average of r-value and not its anisotropy). One suitably designed EMAT generates and detects all the necessary waves. Because the EMAT aperture is small, fixturing is simplified; it is only required to keep the sheet a few mm from the transducer. Furthermore, an error analysis shows that errors as large as three times the "error budget" of the guided wave system can be tolerated.
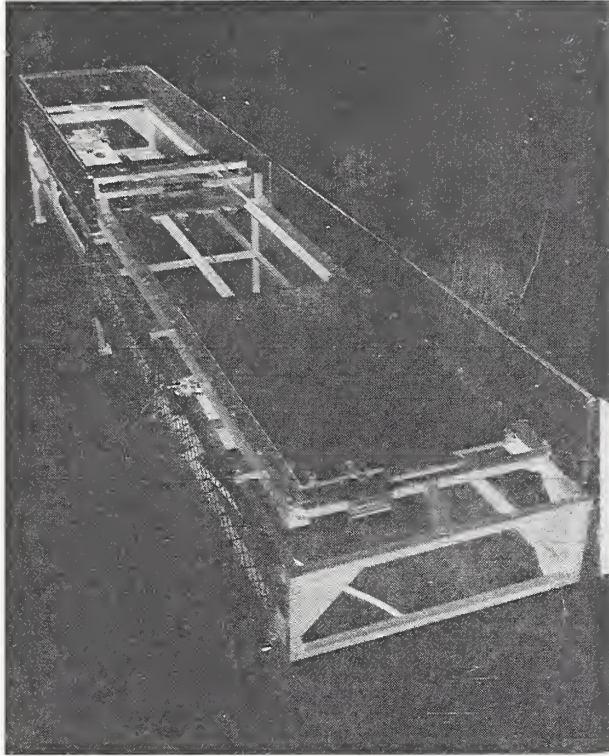
4

Fig. 1. Moving sheet device.

While EMATs have the advantage of noncontact operation, they are less efficient than conventional ultrasonic transducers. Because they act as inductive pickup coils on reception, they also have self-resonances which limit their bandwidth. These are problems we have overcome in our work on the single-EMAT system. To overcome the first difficulty, we use a resonance technique which works well on our thin sheet samples (thickness about 1 mm). Obviously, by resonating the sheet we greatly enhance the signal-to-noise ratio in our measurements. The resonances of the sheet are measured and correlated to $\bar{r}$, as described later. A simplified block diagram of our resonance measurement system is shown in Fig. 2. It is the result of a collaboration research and development agreement between the Materials Reliability Division and a commercial instrument builder (RITEC, Warwick, R.I.). The gated amplifier drives the EMAT with a long toneburst with center frequency ω_F. Assume ω_F is close to a resonant frequency, ω_R. The amplitude of particle displacement builds up to a maximum value determined by attenuation in the sheet. Then, after the toneburst ends, the sheet "rings down" at frequency ω_R. This is detected by the EMAT and amplified. The signal (now with center frequency ω_R) is multiplied by a sinusoid with frequency $\omega_F + \omega_{IF}$, implementing superheterodyne operation. The result is to shift the frequency spectra to $\omega_{IF} + (\omega_F \pm \omega_R)$. The higher frequencies are removed in the IF amplifier and band pass filter stage, leaving frequencies centered at $\omega_{IF} + \omega_F - \omega_R$. The signal is then multiplied by sinusoid at frequency ω_{IF} and low-pass filtered to leave a decaying sinusoid at "beat frequency" $\omega_F - \omega_R$. This is integrated to improve signal-to-noise.

The present resonance measurement instrument operates up to 7.5 MHz with a wide dynamic range. By superheterodyning, critical components of the IF amplifier and subsequent stages need only be designed to work in a narrow frequency range about ω_{IF}. To increase the bandwidth, we have done

5
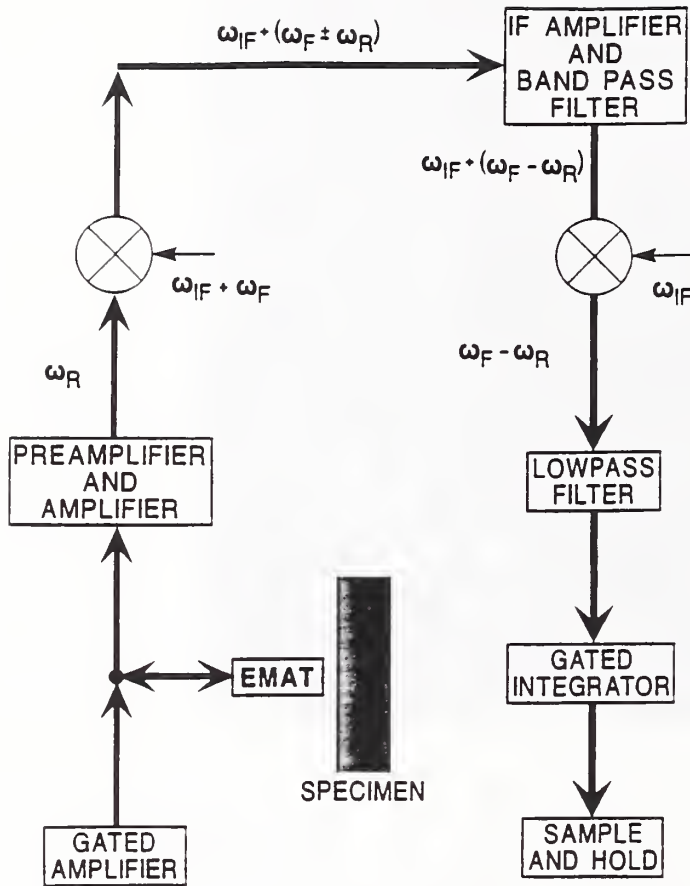
Fig. 2. Simplified schematic illustrating method of resonance measurement of average r-value.

the following. The r.f. coil was designed to have both small inductance and a large number of ampere-turns. The former design criterion caused the EMAT bandwidth to be large; the latter enhances the eddy current $\underline{J}$ in the sample. The magnetic circuit which applies the static magnetic induction was analyzed both with semi-empirical formulas and with a finite element program. The results were used to optimize the circuit to provide a large magnetic induction B, to generate the desired wave types (shear and longitudinal). Hence, we increase the forcing function $\underline{J}$ x $\underline{B}$. The EMAT self-resonance is now above the upper limit of our present electronics.

Modeling of the effect of texture on velocity and on r-value shows that there should be a relation between $\bar{r}$ and the ultrasonic parameter K:

$$K = \frac{V_{RD}^2 + V_{TD}^2}{V_{RD}^2 + V_{TD}^2 + V_L^2} .$$

(1)

Here V_{RD}, V_{TD} are velocities of shear waves polarized along the rolling and transverse directions; V_L is the velocity of a longitudinal wave. Because the transducer generates all waves simultaneously, and these propagate through the same thickness, the ratios of velocities in (1) can be replaced by ratios of resonant frequencies. Resonant frequencies were measured on sheets with known r-values (from mechanical tests). A good correlation between $\bar{r}$ and K was found [4].

REFERENCES

1.   A. V. Clark and Y. Berlinsky, "Effect of Liftoff on Accuracy of Phase Velocity Measurements Made with Electromagnetic-Acoustic Transducers," submitted to Res. in Nondest. Eval.

2.   A. V. Clark, Y. Berlinsky, N. Izworski, Y. Cohen, D. V. Mitrakovic, and S. R. Schaps, "Methods to Improve the Accuracy of On-line Ultrasonic Measurement of Steel Sheet Formability," submitted to J. Nondest. Eval.

3.   A. V. Clark, N. Izworski, Y. Berlinsky, Y. Cohen, and D. V. Mitrakovic, "Proof-of-Concept of On-line Ultrasonic Measurement of Steel Sheet Formability," submitted to Res. in Nondest. Eval.

4.   A. V. Clark, C. M. Fortunko, M. G. Lozev, S. R. Schaps, and M. L. Renken, "Determination of Steel Sheet Formability Using Wideband Electromagnetic Acoustic Transducers," submitted to Res. in Nondestr. Eval.

Thermomechanical Processing of Steels

Yi-Wen Cheng (303-497-5545) and P. T. Purtscher
Materials Reliability Division, Materials Science and Engineering Laboratory

The objectives of this research program are to generate basic metallurgical data and to develop, improve, or validate process models that are needed in the intelligent processing of steels. Thermomechanical processing (TMP) is a continuous process for producing steel products by controlling the time-temperature-deformation schedule during hot working such that the product properties in the as-fabricated condition equal or exceed those of heat-treated grades. The key to improving TMP is intelligent control of the time-temperature-deformation schedule used in hot working. Basic metallurgical data and process models are two of the ingredients that are required in implementation of intelligent processing. Currently, with a few exceptions, models used in the industry are qualitative and empirical. Research is needed to experimentally verify and improve these models and to develop new ones based on physical principles. Verification, improvement, and development of models all need basic metallurgical data.

During FY 1992, the efforts have been on (1) the development and validation of a model that describes the stress-strain behavior at high temperature and high strain rate, (2) the validation of models that describe structure-property relations, and (3) the preparation of a proposal, "Microstructural Engineering in Hot-Strip Mills," which was submitted to American Iron and Steel Industry (AISI); this proposal has been approved by AISI and the Department of Energy.

In the study of items (1) and (2), we have investigated an air-cooled (as opposed to quenched and tempered) Nb-treated microalloyed bar steel, which is being evaluated at Chrysler Motors Corporation to replace the conventional quenched-and-tempered grade. To determine the stress-strain behavior, cylindrical specimens were compressed at temperatures of 900, 1000, 1100, and 1200 °C and constant strain rates of 0.1, 1, and 10 s^{-1}. The results show that, for the Nb-treated microalloyed steel, the flow stress decreases with increasing testing temperature. The flow stress also decreases with decreasing strain rate, except in the case when precipitation occurred at 900 °C with the strain rate of 0.1 s^{-1}. In the latter case, the flow stress is higher than that of testing at the strain rate of 1 s^{-1}. Typical results showing the effects of temperature on the flow stress are presented in Fig. 1. Figure 1 shows typical results of the effects of temperature on flow stress. As shown in the figure, the flow stress increases with decreasing temperature. At a strain equal to 0.3, the true stress (flow stress) increases from about 50 to 150 MPa when the temperature decreases from 1200 to 900 °C.

A mathematical equation, $\sigma = \sigma_s [1 - \exp(-B\epsilon)]^n$, has been developed to describe the high-temperature stress-strain behavior [1]. In the equation, σ is stress, ϵ is strain, σ_s, B, and n are constants that are determined experimentally. Physically, σ_s is the saturation stress, B is related to the characteristics of strain hardening and dynamic recovery, and n is the functional relationship between stress and dislocation density. The combined effects of temperature and strain rate are described by the equation, $[\sinh(\alpha\sigma_s)]^m = A \dot{\epsilon} \exp[\Delta H/(RT)]$ [2], where α, m, and A are constants, $\dot{\epsilon}$ is strain rate, and ΔH is the activation energy of deformation. A computer program has been written to predict the stress-strain behavior with inputs of temperature and strain rate. Without microstructural changes during deformation, such as dynamic precipitation and recrystallization, predictions of the computer program agree well with the experimental data. However, discrepancies exist between predictions and experimental data when precipitation occurred during deformation. Figures 1 and 2 shows the comparison between computer predictions and experimental results.
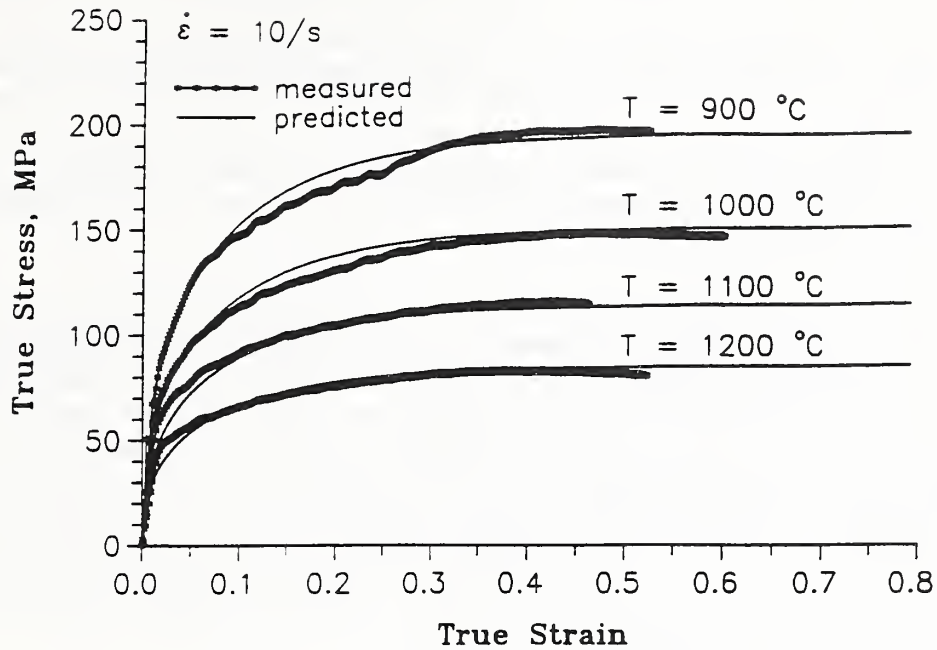
Fig. 1. Effects of temperature on flow behavior of a Nb-treated microalloyed 1141 steel.
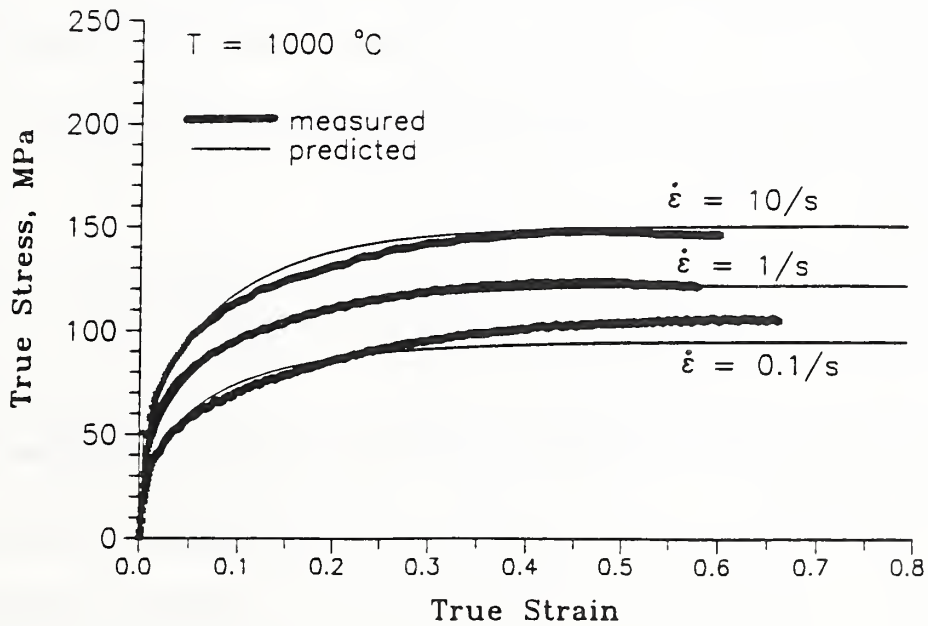

Fig. 2. Comparison of predicted and measured stress-strain curves of a Nb-treated microalloyed steel. The underprediction at the strain rate of 0.1/s is probably due to the occurrence of dynamic precipitation during deformation.

9

In the study of structure-property relationships, the Nb-treated microalloyed steel was processed according to different TMP schedules with a newly upgraded 500-kN TMP simulator to produce different microstructures. Tensile and impact (Charpy V-notch specimens) properties were measured on the specimens extracted from the TMP processed steels. Preliminary results indicated that the equations of Gladman and Pickering [3] predict the tensile properties well when the ferrite content is less than 15% of the structure: the predicted and the measured yield strength were 464 and 471 MPa, respectively, and the predicted and the measured ultimate tensile strength were 795 and 754 MPa, respectively. However, for a ferrite content of 40%, the equations underpredicted the measured values: 20% in yield strength and 11% in ultimate tensile strength.

In the course of conducting TMP research on steel, extensive interactions with researchers in the steel industry have been established and maintained. We worked very closely with the American Iron and Steel Institute (AISI) in preparing the proposal, "Microstructural Engineering in Hot Strip Mills," which is one part of the AISI's Advanced Process Control Program for the steel industry. The objective of the AISI program is to enhance the competitiveness of the North American steel industry in the global market. The microstructural engineering project, which will be performed by a research team consisted of NIST, US Steel and the University of British Columbia (Canada), will develop a predictive tool that can quantitatively link the properties of hot-rolled products to the process parameters of a hot-strip mill. The AISI's program has been approved by the Department of Energy for funding. In addition to AISI, industrial contacts also include Chrysler Motors Corporation, Inland Steel Company, North Star Steel Company, and Republic Engineered Steels, Inc.

REFERENCES

1.   Y. W. Cheng and R. M. Kuziak, "High-Temperature and High-Strain Rate Flow Behavior of a Nb-Treated Bar Steel," presented at the 33rd Mechanical Working and Steel Processing Conference, St. Louis, MO., Oct. 20-22, 1991.

2.   J. J. Jonas, C. M. Sellars, and W. J. McG. Tegart, Metallurgical Reviews, pp. 1-24, 1969.

3.   T. Gladman and F. B. Pickering, in: Yield, Flow and Fracture of Polycrystals, ed. T. N. Baker, Applied Science Publishers, Ltd., London and New York, pp. 141-198, 1983.

PUBLICATIONS

1.   Y. W. Cheng and R. M. Kuziak, "High-Temperature and High-Strain Rate Flow Behavior of a Nb-Treated Bar Steel," presented at the 33rd Mechanical Working and Steel Processing Conference, St. Louis, MO., Oct. 20-22, 1991, to be published.

2.   P. T. Purtscher and Y. W. Cheng, "Structure-Property Relationships in Microalloyed Ferrite-Pearlite Steels, Phase 1: Literature Review, Research Plan, and Initial Results," NISTIR 3992, August, 1992.

Magnetic Methods for Determination of Mechanical Properties of Steel

L. J. Swartzendruber (301-975-6034) and G. E. Hicho
Metallurgy Division, Materials Science and Engineering Laboratory

The objective of this investigation is to improve and extend the applicability of magnetic sensing methods to determining the mechanical properties of steel during processing. To meet this objective we have previously investigated the mechanical and magnetic properties of several samples of steel sheet and shown that correlations could be found between selected mechanical properties and the magnetic Barkhausen signal. This is somewhat expected since Barkhausen signals are produced by impediments to the rotation of magnetic domains. These are caused by metallurgical microstructures that also correlate with mechanical properties. To further explore these and other relationships, it was decided to use samples of steel sheet obtained directly from a steel mill. Hence, a trip was taken to the Middletown Works of Armco Steel Company in order to observe sheet mills in action and to select various samples of rolled sheet that could be investigated both for metallurgical and magnetic properties. Applicable rolled sheet specimens were selected by Armco engineers and sent to NIST. In order to have comparative test results, both Armco and NIST metallurgists measured the mechanical properties and performed metallographic examinations.

A general description of the steels supplied by Armco Steel Corporation is shown in Table 1. These steels were picked primarily because they are produced in large quantities and generate considerable scrap which could be reduced by improved process control. Six of the seven steels were batch annealed and one was continuous annealed.

TABLE I
General Description of Steel Samples

Sample	Condition(1)	Type	HRB
CR7	CR BA	Low Carbon	34.0
CR8	CR BA	Low Carbon	35.0
IF16	CR BA	Interstitial Free, Ti & Nb Stabilized	35.7
IF17	CR BA	Interstitial Free, Ti Stabilized	20.0
IF18	CR BA	Interstitial Free, Ti Stabilized	20.0
ZG4	HDG CA	Ultra-Low Carbon	38.1
ES7	EG BA	Interstitial Free, Ti Stabilized	34.0
(1) CR = Cold Rolled, BA = Batch Annealed, CA = Continuous Annealed, EG = Electrogalvanized, HDG = Hot-Dip Galvanized			

Metallurgical examination of the low carbon steel specimens, CR7 and CR8, showed the steel was primarily ferrite with carbides dispersed throughout the ferrite. The interstitial free steel IF16, which was both titanium and niobium stabilized, had a microstructure of primarily ferrite with no resolvable
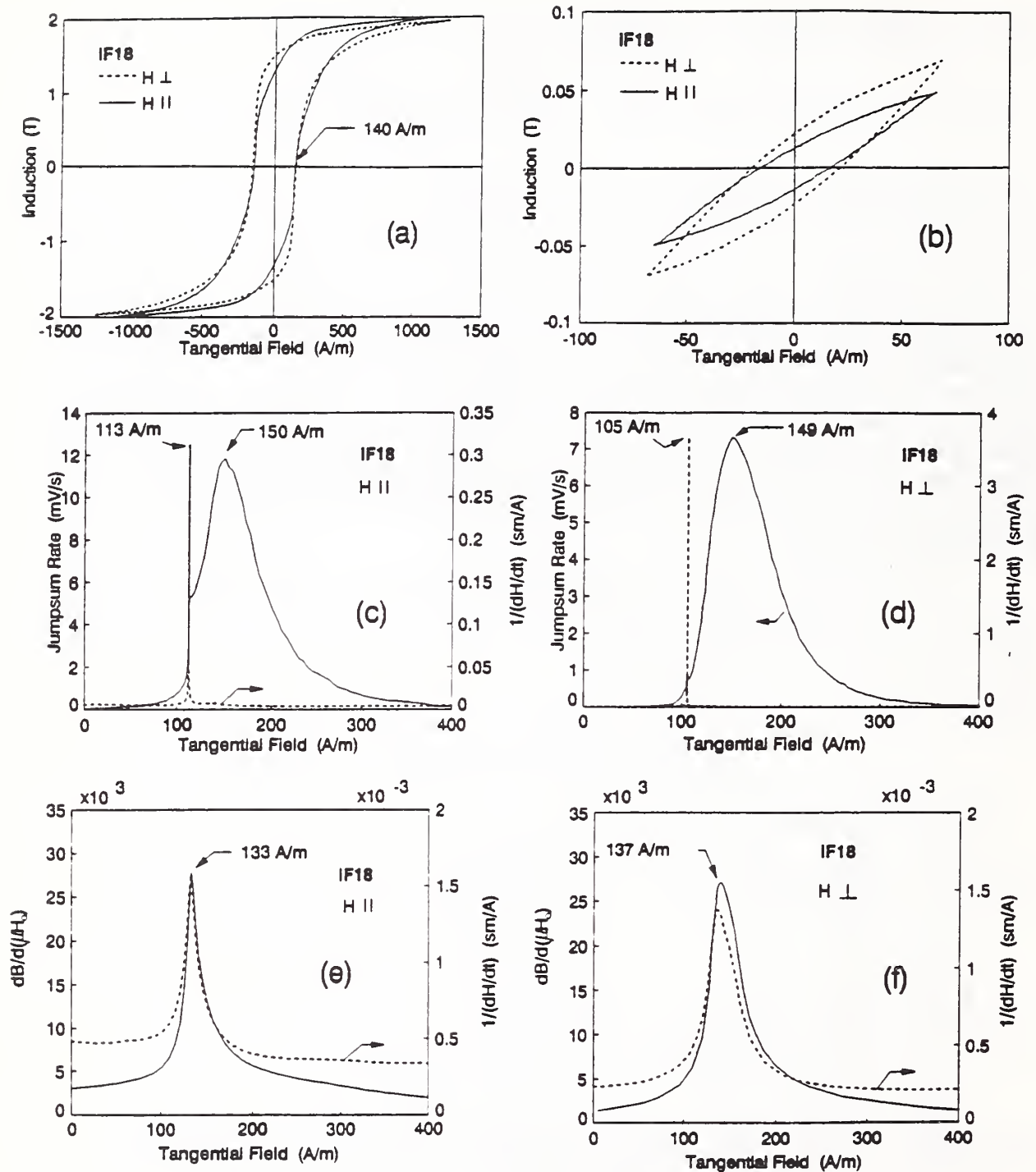
Fig. 1. Magnetic properties observed for sheet steel sample IF18. (a) Full hysteresis loops for H applied parallel (solid line) and perpendicular (dotted line) to the rolling direction. (b) The small field, or initial, hysteresis loops. (c) The Barkhausen jumpsum rate and the inverse of dH/dt for H applied parallel to the rolling direction. (d) The Barkhausen jumpsum rate and the inverse of dH/dt for H applied perpendicular to the rolling direction. (e) and (f) The slopes of the hysteresis loops and the inverse of dH/dt determined from the data of Figure 1(a).

12

Fig. 2. Correlation of yield strength (0.5% offset) and coercive force determined for the samples listed in Table 1.

carbides at 100x magnification. Similar microstructures were found for the other two interstitial free steel specimens, IF17 and IF18, which were only titanium stabilized. There does appear, however, to be some unresolvable carbide present in the ferrite for these two samples. The microstructure of the electrogalvanized steel consisted of elongated ferrite, and the absence of carb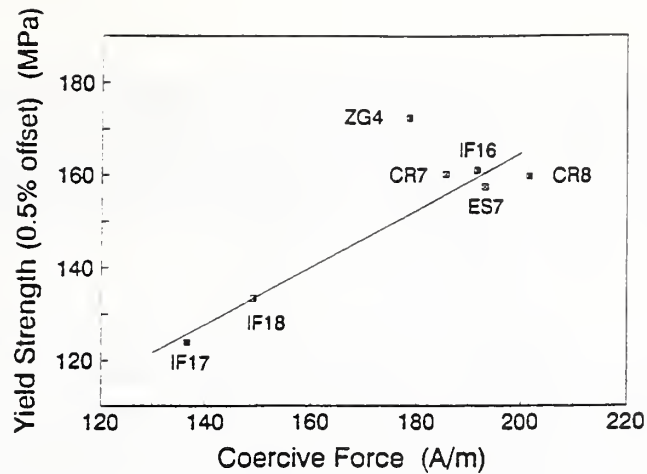ides in the ferrite was noted since the steel was titanium stabilized. The hot-dipped galvanized sample had a microstructure consisting of ferrite with fine carbides dispersed throughout. The grain sizes observed were between 7 and 8 (ASTM grain size).

The magnetic properties measured for each sample were the Barkhausen signal spectrum, the coercive force, the initial susceptibility, the incremental susceptibility as a function of applied field, and the time rate of change of the tangential magnetic field as the flux through the sample was changed at a uniform rate. Each property was measured both parallel and perpendicular to the rolling direction of the samples. Figure 1 shows a set of measurements on sample IF18. The hysteresis loops shown in (a) and (b) of Figure 1 were taken at 0.5 Hz using an encircling coil as a detector. The relative permeability, $dB/d(\mu_o H)$ in Figure 1 (e) and (f), was determined from the full hysteresis curve, Figure 1(a). The initial susceptibility was estimated from the low field loop, Figure 1(b). The inverse of dH/dt, where H is the tangential component of the magnetic field measured using a Hall probe at the sample surface, is plotted as a dotted line in Figures 1(c), (d), (e), and (f). Note that these curves are much sharper and occur at lower field in (c) and (d). This is because the curves in (c) and (d) were obtained at 0.025 Hz while the Barkhausen spectrum was being obtained, whereas the curves in (e) and (f) were obtained at 0.5 Hz while the hysteresis loop was being obtained. Note that the peak in 1/(dH/dt) occurs very close to the coercive force. This is of interest because the hysteresis loops can not be determined in an on-line measurement, whereas dH/dt can. Figures 1(c) and 1(d) show the Barkhausen signal (solid line, plotted as the "jumpsum rate"). Of particular interest in these signals are their moments which are related to the hysteresis loop shapes.

The mechanical properties determined for each sample were the yield strength, at both 0.2% and 0.5% offset, the hardness, the ultimate tensile strength, and the percent elongation. Hardness values are given in Table 1. Note that the batch annealed sample, which is coiled colder at the hot-strip mill than the continuous annealed material, has a high hardness in spite of its low-carbon content. A comparison of the hardness results for all the interstitial free steel samples revealed that sample IF16, titanium and niobium stabilized, was harder, HRB 35.7, than the interstitial free steel samples IF17 and IF18 (HRB 20.0 and 20.3). This appears to be due to the ferrite size observed for these steels. Samples IF17 and IF18 were found to have ferrite grains that were coarser than sample IF16.

13

Correlations between the magnetic and mechanical properties were investigated. It was found that, for all samples, the yield strength and hardness were related. The yield strength and a number of magnetic properties, including initial susceptibility, first and second moments of the Barkhausen noise spectrum, and coercive force, were closely correlated except for sample ZG4, the continuous annealed sample. Figure 2 shows a plot of the yield strength as a function of the coercive force. Note that the batch annealed sample, ZG4, is off the general trend line.

In the course of conducting this magnetic sensor research for steel processing, extensive interactions with the steel industry have been established and maintained. We have worked closely with the American Iron and Steel Association (AISA) in preparing a proposal which is one part of the AISI's Advanced Process Control Program for the steel industry. The object of the AISI program is to enhance the competitiveness of the North American steel industry. Our project on magnetic sensing is part of a task to develop on-line sensing techniques. In this task, which will begin in FY 1993 with Department of Energy support, we are teamed with the National Research Council of Canada (ultrasonic sensors) Armco Steel Company and two commercial sensors manufacturing companies, Data Measurement Corporation and Ultas - Optec Inc. (a Canadian company).

Initial work will center on procurement of a well characterized set of sheet steel samples which cover a wide range of mechanical properties. This set will be used to determine if relationships between the magnetic and mechanical properties are sufficiently valid in a statistical sense to be useful as a tool in the intelligent processing of sheet steel.

During the current period a study was made of the relationship between transducer configuration and the observed magnetic Barkhausen observations. A number of characteristics of the Barkhausen signal, including power density, autocorrelation, jumpsum density, and noise emission rates, were obtained with different transducer types on low-carbon sheet steels. Four different transducer arrangements were used: a tightly wound small encircling coil, a large loosely wound encircling coil, a surface coil, and a surface transducer fabricated from a ferrite core. It was found that the rms voltage and jumpsum properties were nearly the same for all these transducer arrangements. In particular, the surface coil and encircling coil, when properly configured, gave nearly identical results even though the strength of the Barkhausen signal coupled into the surface coil was smaller than for the encircling coil.

When the hysteresis loop was transversed using a constant rate of flux change, the peaks in the Barkhausen signal occurred at a field which was near, but slightly less than, the coercive force of the material. These results will be useful when designing transducer systems for on-line use.

PUBLICATION

1.   L. J. Swartzendruber and G. E. Hicho, "Effect of Transducer Configuration on Magnetic Barkhausen Observations," Research in Nondestructive Evaluation, **4**, Issue 3, (1992).

Ultrasonic Sensing of Liquid/Solid Interfaces in Metals

W. L. Johnson (301-975-6144), J. B. Spicer, and S. J. Norton
Metallurgy Division, Materials Science and Engineering Laboratory

The mechanical properties of metallic alloys are strongly dependent on the microstructure which evolves as the material is solidified. The importance of understanding and controlling the process of solidification in metals has led to considerable theoretical and experimental effort. Unfortunately, these efforts have been hampered by a lack of sensors which can provide real-time information on solidifying interfaces in opaque materials. The experimental verification of theoretical models has relied primarily on studies of transparent materials and metallographic analysis of fully solidified metals.

This on-going project seeks to develop ultrasonic techniques for providing information on both the position and structure of liquid/solid interfaces in directionally solidifying metals. Since ultrasonic wavelengths are comparable to typical dimensions of interface structures (e.g., dendritic arm spacings), the angular and frequency dependence of waves scattered from an interface will contain information about these structures. Ultrasonic waves propagating through solid polycrystalline metals can be strongly scattered by grain boundaries. Because of this, a wave which is scattered off a liquid/solid interface after propagating through the solid is unlikely to provide useful information on the structure of the interface. A liquid, on the other hand, is an ideal isotropic medium in which to perform scattering studies. In order to take advantage of this fact, an ultrasonic interface sensor must generate ultrasonic waves in the liquid and, then, receive the waves in the liquid after they have been reflected by the interface. This is the approach which is being pursued here.

Past work on this project explored various transduction configurations, including magnetostrictive wire waveguides with coil sensors, laser generation, and interferometric detection. Ultrasonic waves reflected from an interface between liquid tin and stainless steel were successfully detected using a configuration which employed lasers for both generation and detection. Ultrasonic waves scattered from periodic structures in water were studied experimentally and theoretically in order to explore general techniques which might be used in analyzing waveforms reflected from interfaces. An ultrasonic technique for measuring the resonant frequencies of spheres was developed for the purpose of providing ultrasonic data on metallic droplets undergoing solidification [1].

During FY 1992, the research effort has been directed primarily towards characterizing the laser source in order to facilitate the design of an improved sensor which uses laser generation and detection. The apparatus shown in Figure 1 was used to study waveforms as a function of angle with respect to the axis of the source. A 6.5-mm-diameter pulsed Nd:YAG beam was passed through a pair of rotatable silica rods which were designed such that the tin/silica interface where the ultrasonic wave was generated could be tilted with respect to the axis of the crucible. A He:Ne interferometer detected the wave at the bottom through a silica rod.

An understanding of the dominant features of the received broadbanded ultrasonic waveforms has been attained from calculations which have been performed using thermoelastic theory [2]. The angular dependence of the amplitude of the received waveforms is, also, close to that predicted by theory. Perhaps, the most significant feature of the data, from the perspective of designing an ultrasonic sensor, is that the wave is found to be directed within just a few degrees of the source axis.
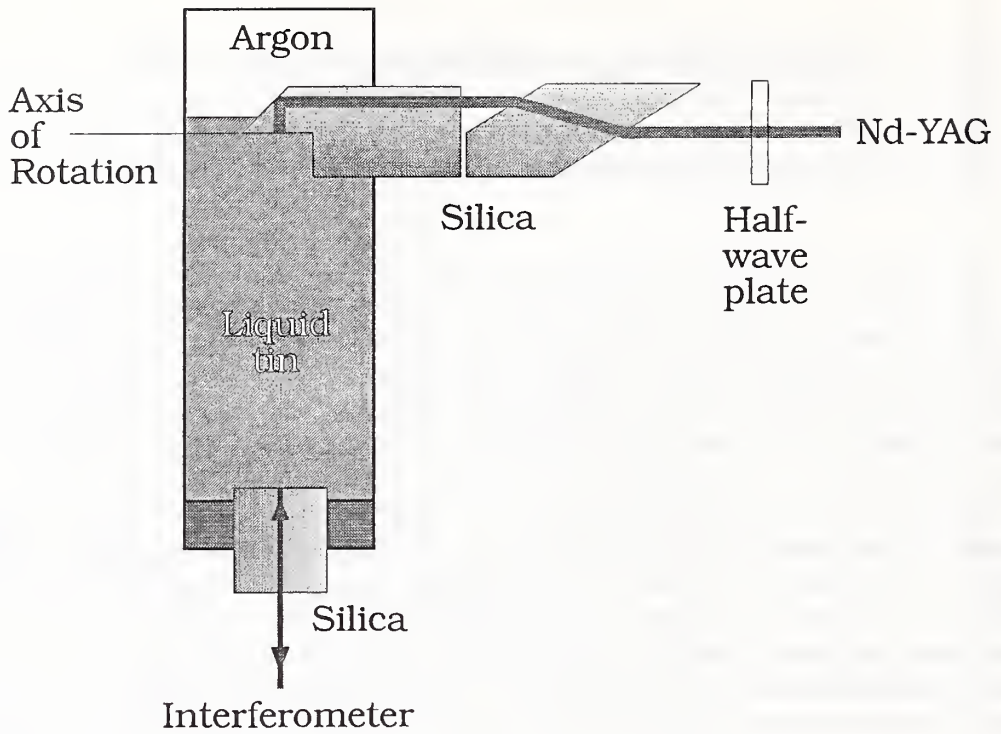
Fig. 1. Apparatus used to study the characteristics of laser-generated ultrasonic waves in liquid tin. The waves are generated by a Nd:YAG beam at the interface between the tin and the silica at the top of the crucible. This interface can be tilted with respect to the axis of the crucible. A He:Ne interferometer detects the transmitted wave.

Fig. 2. Apparatus used to study ultrasonic waves reflected from a liquid/solid tin interface. The tin solidifies from the bottom when the base is cooled with air.

Fig. 3. Waveforms received with the apparatus shown is Fig. 2. (a) Reflection off the stainless base with the tin fully liquid. (b)-(d) Sequential waveforms as the tin solidifies from the bottom; the reflection from the liquid/solid tin interface (the first received pulse) can be seen advancing in time as the interface moves upward.

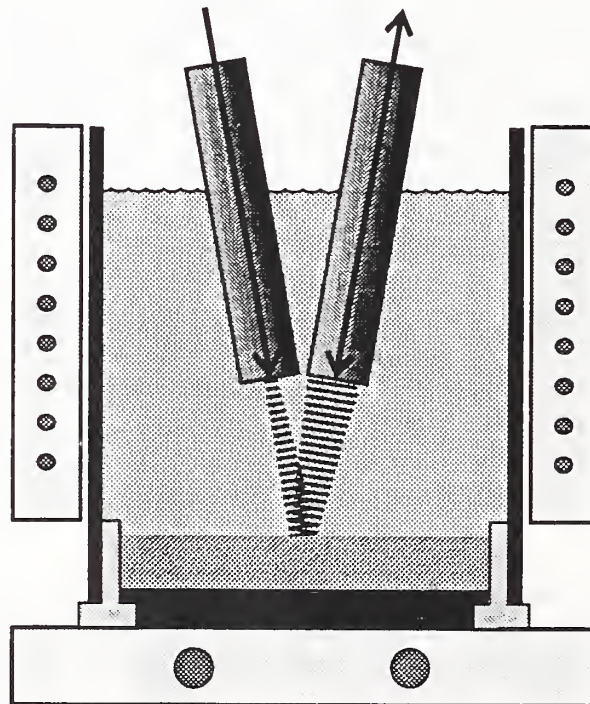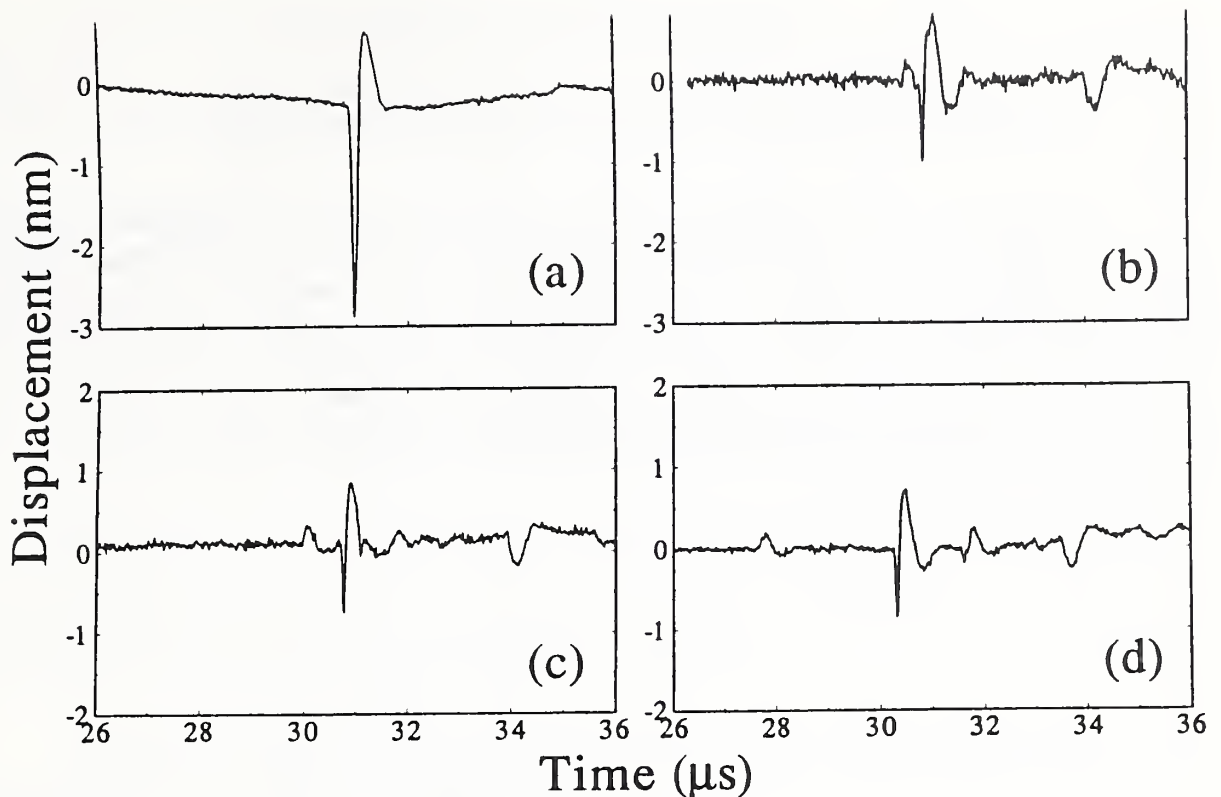A configuration which provides for detection of reflected ultrasonic waves is shown in Figure 2. The two immersed silica rods, through which laser generation and detection is accomplished, are tilted such that detection is at the angle of specular reflection of the stainless crucible base. Figure 3(a) shows the waveform received after reflection off the tin/stainless interface with the tin entirely liquid. The sequential waveforms in Figures 3(b)-3(d) were obtained as the tin was solidified from the bottom of the crucible by air-cooling the base. The reflection from the liquid/solid tin interface can be seen to advance in time as the interface moves closer to the silica rods.

REFERENCES

1.   Ward Johnson, Stephen Norton, Felix Bendec, and Robert Pless, "Ultrasonic spectroscopy of metallic spheres using electromagnetic-acoustic transduction," J. Acoust. Soc. Am., Vol. **91**, 2637, 1992.

2.   James B. Spicer, "Laser ultrasonics in finite structures: Comprehensive modeling with supporting experiment," Ph.D. thesis, Center for Nondestructive Evaluation, Johns Hopkins University, 1991.

Modeling Detachment in Welding

T. A. Siewert (303-497-3523), T. P. Quinn, and R. B. Madigan
Materials Reliability Division, Materials Science and Engineering Laboratory

The objective of this investigation is to develop process models for droplet detachment for gas metal arc welding (GMAW), for the purpose of improving the control of weld quality. The very high current density (hundreds of amperes per square millimeter) and temperature at the electrode tip make experimental measurements difficult. A better understanding of the droplet detachment and process models was developed and confirmed with experimental measurements permitting the behavior in this region to be deduced. Based on the models, we will be developing intelligent processing strategies and selecting appropriate sensing techniques and control systems to improve the quality of welds produced with automated GMAW systems.
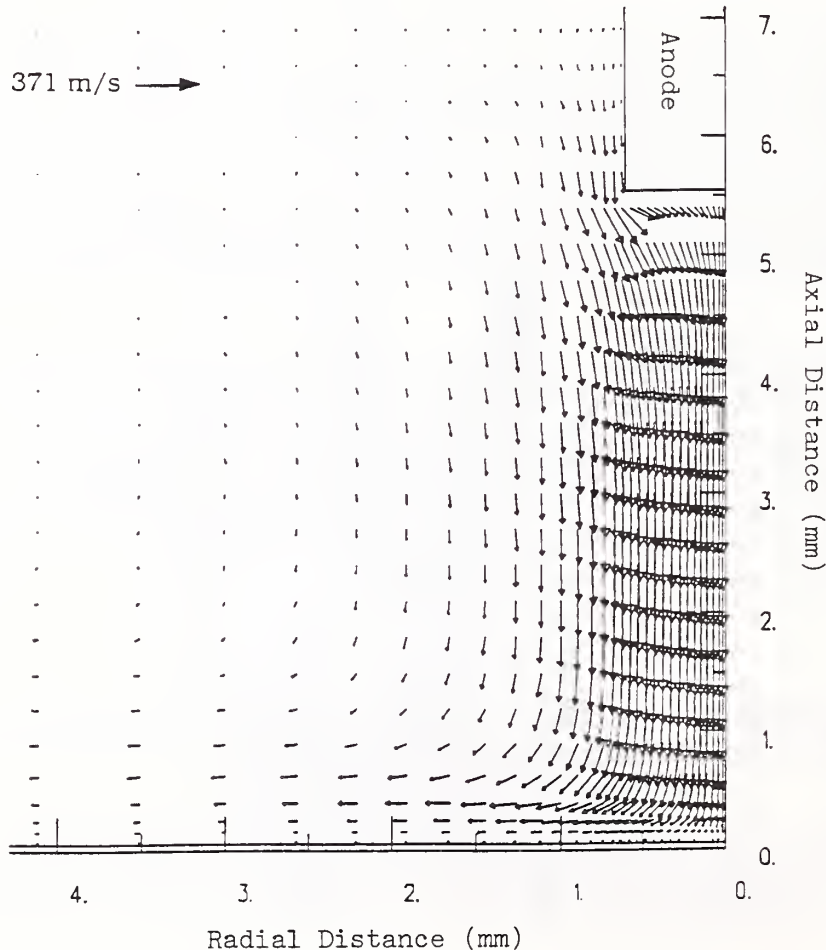

Fig. 1. The gas velocity in an argon arc during GMAW for a current of 250 A and a cathode spot size of 2.5 mm.

During this year, a steady state model of the arc during gas metal arc welding was developed with NIST support by Par Jonsson (a Massachusetts Institute of Technology graduate student working at NIST during the summers) and Professor Julian Szekely at the Massachusetts Institute of Technology. The fundamental transport equations for the radial and axial velocities, pressure, enthalpy and electric potential have been solved, accounting for the temperature dependent physical properties of the shielding gas (argon). The geometries of the electrode and weld pool as well as the overall process variables (current, electrode feed speed, etc.) used in the model were measured in experiments carried out in the NIST Welding Test Bed. Figure 1 shows the predicted gas velocity in a steady state GMAW argon welding arc. Future work will include (1) calculations with a tapered anode (the tip of the melting electrode) using the dimensions measured in the experiments and (2) calculations of the geometry of the fluid film at the end of the electrode to predict droplet detachment.

Also during this year, a dynamic model of the melting electrode during GMAW was completed [1, 2]. The model considered the heat sources of Joule heat in the electrode and heat directly applied to the end of the electrode by the condensing electrons, and heat loss by conduction along the electrode. The thermal conductivity, the thermal diffusivity, and the electrical resistivity of the electrode material were allowed to vary with temperature. The model was verified with experiments. The steady state electrode extension can be predicted within 1.9 mm. The model is a transient version of the steady state model proposed by Kim et al. [3] and has allowed for the development of quasi-linear transfer functions relating electrode extension to electrode feed speed and current.

The melting electrode model together with the model of the arc allows for a thorough theoretical description of the process current-voltage characteristics. These models provide valuable support for our development of new weld sensing strategies [4-5].

REFERENCES

1.   T. P. Quinn, R. B. Madigan, and T. A. Siewert, "An Electrode Extension Model for Gas Metal Arc Welding," submitted to Welding Journal.

2.   T. P. Quinn, R. B. Madigan, and T. A. Siewert, "An Electrode Extension Model for Gas Metal Arc Welding," Document SG212-793-91, International Institute of Welding, available from the American Council of the IIW, American Welding Society, Miami, Florida, 1992.

3.   Y.-S. Kim, D. M. McEligot, and T. W. Eagar, "Analysis of Electrode Heat Transfer in Gas Metal Arc Welding," Welding Journal, 70, No. 1, 20-s, 1991.

4.   T. A. Siewert, R. B. Madigan, T. P. Quinn, and M. A. Mornis, "Through-the-Arc Sensing for Real-Time Measurement of Gas Metal Arc Weld Quality," submitted to Proc. Computerization of Welding Information Conference, American Welding Society, Miami, Florida, 1992.

5.   R. B. Madigan, T. P. Quinn, and T. A. Siewert, "Sensing Droplet Detachment and Electrode Extension for Control of Gas Metal Arc Welding," submitted to Recent Trends in Welding Science and Technology, ASM International, Materials Park. Ohio, 1992.

Polymer Blends Processing Modeling

C. C. Han (301-975-6772)
Polymers Division, Materials Science and Engineering Laboratory

The objective of this effort is to understand the variables controlling the mixing/demixing kinetics which are critical in all polymer blends/alloys processes designed to control the structure and morphology of the final material and its tailored properties. The multivarient model obtained can be used to guide new product development and hopefully in the future be used as part of an intelligent processing system for on-line control.

The use of polymer blends/alloys has proliferated in recent years, especially in civilian commerce and consumer products. This is one of a few areas which has maintained growth even during economic recessions. The reason for the growth is simply due to the low investment in production cost for materials with new properties. The wide spectrum of properties obtained through the synergistic effect of alloying provided engineering flexibility. Although the investment costs of the final product is not very high, the combination of the value enhancement and total sales of new polymer blends and alloys in the commercial market lead to enormous added value. These engineering materials may not be considered as high performance materials in terms of the ultimate use temperature, strength and modulus, but the science/technology involved in producing these blends, resins, films, fibers, etc. can be very demanding. These are certainly high technology materials which have made significant impact on our every day life. The science/technology involved can be categorized as follows:

1. Thermodyanmics of the polymer blends: includes the binary interaction parameters and free energy of mixing for the binary system [1], and the copolymer effect on the phase behavior [2-5].

2. Kinetics of phase separation: this is the key step in morphological control, which includes spinodal decomposition, nucleation and growth and late stage coarsening effects [6-8].

3. Effects of crosslinking and grafting on the thermodynamics and kinetics: includes effects such as stabilization and/or enhancing phase separation through crosslinking [9-10]; morphology stabilization through inter-chain crosslinking and grafting.

4. Shear mixing/demixing and phase separation kinetics after cessation of shear: this process models the actual mixer/extruder operation in any blending/alloying process [11-12]. This is a crucial part of the whole effort; however, information obtained from (1) and (3) is necessary in modeling this process.

5. Interfacial modification and control: interfacial modification and control of phase separated polymer blends/alloys determine the final mechanical properties and stability of the material. This modification can also influence the kinetics of coarsening as well as the mixing/demixing processes. Items (4) and (5) are least understood in this important field where empirical approaches are leading science/technology at the present time.

We have been studying items (1), (2), (3), and (4) in previous years through various support. In the current effort (started this year) we emphasize items (4) and (5). We organized a workshop in April, 1992 and obtained initial agreements from several companies to join a NIST/Industry Consortium to study the morphology and interface control and characterize industrially relevant blends. We are

aiming to initiate this consortium in late 1992. The results of the consortium research will be used as a model by member companies for further development of their company's specific blends/alloys.

Some preliminary studies have been carried out on polydiene blends [2-5], polyolefin blends [13] and polystyrene/poly-butadiene blends [14-15] for their feasibility as a model system to be used for a consortium study. The final selection will be decided by the consensus of all committed member companies.

REFERENCES

1. Temperature, Composition and Molecular Weight Dependence of the Binary Interaction Parameter of Polystyrene/poly(vinyl-methylether) Blends, C. C. Han, B. J. Bauer, J. C. Clark, Y. Muroga, Y. Matsushita, M. Okada, Q. Tran-Cong, T. Chang and I. C. Sanchez, Polymer, **29**, 2002, 1988.

2. Microstructure and Isotopic Labeling Effects on the Miscibility of Polybutadiene Blends Studied by the SANS Technique, S. Sakurai, H. Hasegawa, T. Hashimoto, I. G. Hargis, S. L. Aggarwal and C. C. Han, Macromolecules, **23**, 451, 1992.

3. SANS and LS Studies on the Miscibility of Protonated Polyisoprene/Deuterated Polybutadiene Blends, H. Hasegawa, S. Sakurai, M. Takenaka, T. Hashimoto and C. C. Han, Macromolecules, **24**, 1813, 1991.

4. Microstructure Effects on the Lower Critical Solution Temperature Phase Behavior of DPB and HPB Blends Studied by SANS, S. Sakurai, H. Jinnai, H. Hasegawa, T. Hashimoto and C. C. Han, Macromolecules, **24**, 4839, 1991.

5. SANS and LS Study on the Miscibility of Poly(styrene-r-butadiene)/poly-butadiene Blends, S. Sakurai, T. Izumitani, H. Hasegawa, T. Hashimoto and C. C. Han, Macromolecules, **24**, 4844, 1991.

6. Dynamics of Concentration Fluctuation in a Polymer Blend on Both Sides of the Phase Boundary, T. Sato and C. C. Han, J. Chem. Phys., **88**, 2057, 1988.

7. Time Resolved SANS in Intermediate and Late-Stage Spinodal Decomposition of DPB/HPI Blends, H. Jinnai, H. Hasegawa, T. Hasegawa and C. C. Han, Macromolecules, **24**, 282, 1991.

8. Spinodal Decomposition in Hydrogen-Bonded Polymer Blend, M. He, Y. Liu, Y. Feng, M. Jiang and C. C. Han, Macromolecules, **24**, 464, 1991.

9. SANS Studies of Compatible Blends of Linear PVME and Crosslinked DPS, B. J. Bauer, R. M. Briber and C. C. Han, Macromolecules, **22**, 940, 1989.

10. Effect of Crosslinks on the Miscibility of a DPB and HPB Blend, H. Jinnai, H. Hasegawa, T. Hashimoto, R. M. Briber and C. C. Han, submitted to Macromolecules.

11. Shear Stabilization of Critical Fluctuations in Bulk Polymer Blends Studied by SANS, A. I. Nakatani, H. Kim, Y. Takahashi, Y. Matsushita, A. Takano, B. J. Bauer and C. C. Han, Polymer, in Press.

12. Anisotropic Phase Separation Kinetics in a Polymer Blend Solution Following Cessation of Shear Studied by LS, D. A. Waldow, A. I. Nakatani and C. C. Han, Polymer, in Press.

13. Thermodynamic Interactions in Model Polyolefin Blends Obtained by SANS, N. P. Balsara, L. J. Fetters, N. Hadjichristidis, D. J. Lohse, and C. C. Han, submitted to Macromolecules.

14. Deviation from Mean-Field Behavior in a Low Molecular Weight Critical Polymer Blend, D. W. Hair, E. K. Hobbie, A. I. Nakatani, and C. C. Han, J. Chem. Phys., **96**, 9133, 1992.

15. Critical Dynamics of an Asymmetric Binary Polymer Mixture, D. W. Hair, E. K. Hobbie, J. Douglas and C. C. Han, Phys. Rev. Lett., **68**, 2476, 1992.

Eddy Current Temperature Sensing

A. H. Kahn (301-975-6146) and L. C. Phillips
Metallurgy Division, Materials Science and Engineering Laboratory

A. Stern, Guest Scientist, Nuclear Research Centre-Negev, Beer-Sheva, Israel

This project on the application of electromagnetic methods to the measurement of temperature of aluminum during processing is a joint effort of NIST and The Aluminum Association, Inc. The electrical resistivity of the material to be tested is a function of temperature, alloying composition, and metallurgical state. Eddy current methods provide a rapid means of performing a non-contact measurement of resistivity during processing [1]. If the effects of composition and state can be accounted for, then the resistivity measurements may be used to obtain an on-line determination of the temperature. The principal objective is to develop a system suitable for monitoring temperature during hot-rolling of aluminum sheet.

To pursue these objectives, a simulation test was planned for studying resistivity vs. temperature and the effect of alloy composition. Aluminum samples were supplied by five manufacturers, each contributing four coils of aluminum sheet with varied compositions. The test was hosted by the Alcan Research and Development Center, Kingston, Ontario; a suitable furnace and transport system was available for studying temperature and speed effects with a number of different sensors. The test was conducted by personnel of NIST, Alcan, and the Data Measurement Corporation of Gaithersburg, MD. To obtain the resistivity measurement from the eddy current sensor, it is necessary to know the thickness of the material being tested. Since this will vary during processing, an on-line thickness gauge is required. A beta-ray attenuation gauge was supplied by the Data Measurement Corporation and integrated into the sensor system. Additional temperature sensors used in the test were contact thermocouples to serve as the temperature referee, and an infrared pyrometer. Figure 1 shows a block diagram of the sensors, computers, controllers, and data flow paths used during the test.
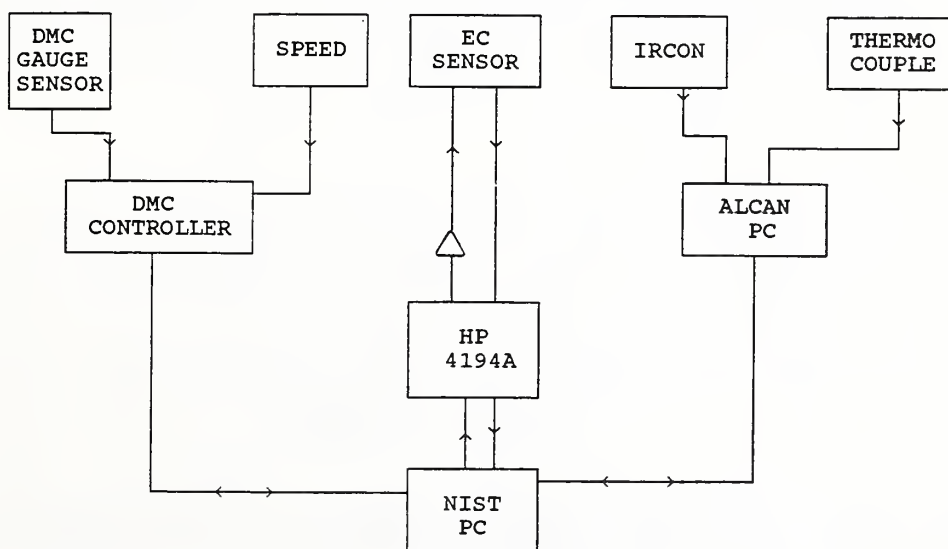

Fig. 1. Configuration of sensors used in the tests reported. The thermocouple readings were manually entered in the DMC controller.

The eddy current sensor is of the through-transmission design previously reported [2]. A primary coil excites eddy currents in the material under test; a secondary coil, on the opposite side of the sample, receives a signal dependent upon the response of the material. A commercial gain-phase analyzer is used to record the transfer impedance of the two coils. The frequency of maximum eddy current dissipation in the test material may be used to obtain a measure of the resistivity [2]. Twenty frequency steps were used, from 800 Hz to 2500 Hz. On-line measurements were begun every two seconds, with an on-screen report occurring four seconds after the start of a measurement. All data were recorded for later analysis. Typical steady temperature runs were of five minutes duration. Temperatures of the test material ranged from 300°C to 400°C.

The coils of aluminum were of thicknesses varying from 0.28 mm to 0.51 mm; the width was 0.28 m and the lengths were approximately 1500 m. The material selected for the test was aluminum alloy 3104. The manganese and magnesium compositions (constant within a coil) were intentionally varied from coil to coil to lie within the alloy specification, but with sufficient spread to allow a test of the sensitivity of the sensor system to composition. Figure 2 shows the range of Mn and Mg compositions in the alloys studied at Kingston.
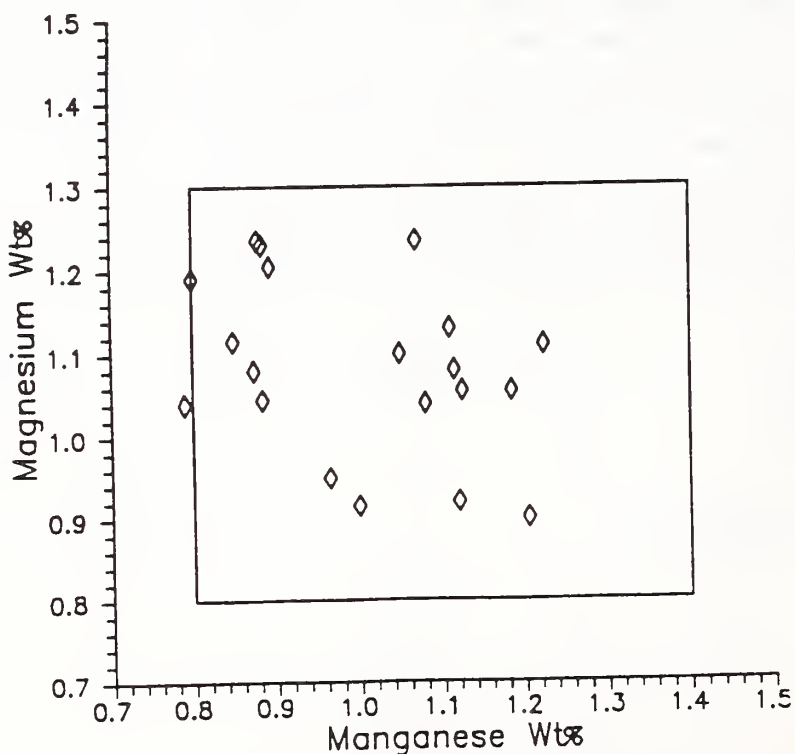

Fig. 2. Range of composition variations of manganese and magnesium in the aluminum coils supplied for the tests. The rectangle indicates the permitted limits for alloy 3104.

A typical final plot of temperature vs. time is shown in Figure 3. The dots represent the eddy current reading, computed as if the resistivity measured were that of pure aluminum, but with a temperature shift added to account for alloying effects. The alloy shifts vary among the many test samples by 150°C to 200°C, approximately. The task of the analysis is to determine to what extent it is possible to account for these alloy shifts in order to use the eddy current data to obtain temperatures.
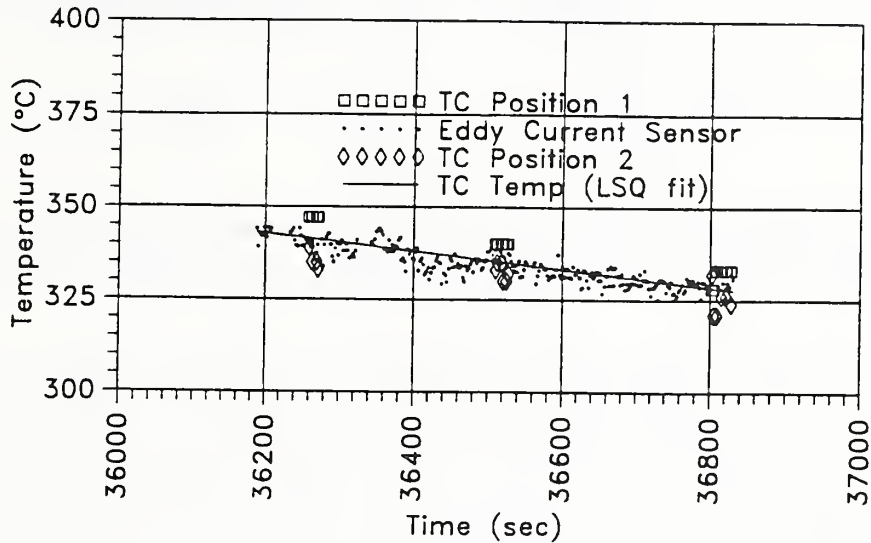

Fig. 3. Typical plot of measured temperatures vs. time for moving material. Thermocouple readings were taken on opposite sides of the eddy current sensor while the sheet was moving.

We analyze the data according to the following scheme. We assume Matthiessen's Rule [3]: "At room temperature and higher, dilute alloys have an electrical resistivity which arises from that of the pure metal with additive contributions from each composition component, deformation, etc." We write

$$\rho_{meas.}(T) = \rho_{pure}(T) + \Delta\rho_{compos.} + \Delta\rho_{deform.} \tag{1}$$

where the resistivity of the pure material is taken from the results of Milek and Welles[4]. At elevated temperatures, we find the resistivity of the alloys is typically of the order of 9 $\mu\Omega \cdot cm$, while that of the pure metal at elevated temperatures is of the order of 7 $\mu\Omega \cdot cm$. From annealing experiments, we find the deformation resistivity is 0.035 $\mu\Omega \cdot cm$ for the grade H18 material supplied. From the shifts in temperature relative to the thermocouple readings, we performed a least squares fit to determine a unique resistivity shift for each alloy of the tests. Then, by measuring room temperature resistivities of these same materials, we obtained an independent set of these resistivity shifts. The high temperature values are plotted against the room temperature values in Figure 4. Error bars indicate 3-sigma variations of the high temperature values based on the use of all measured data. Ideal correspondence to Eq.(1) would require all measured points to lie on a 45 degree straight line passing through the origin. The error bars for the resistivity shifts of Figure 4 correspond to a 3-sigma spread in temperature of $\pm20°C$. Within the limit of error, the Matthiessen condition is met for these alloys.
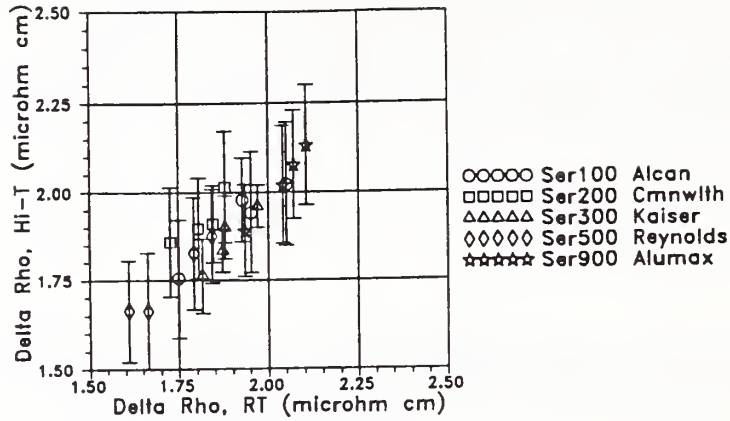
Fig. 4. Resistivity additions due to alloy composition variations. Values computed from high temperature data are plotted against values observed at room temperature. Error bars are 3-sigma ranges. Ideal additivity would require all points to lie on a 45° line through the origin.

A preferable measure of the precision of the temperature measurement is obtained by using Eq.(1) with the resistivity shifts determined at room temperature, and comparing the thermocouple measurements with an average of the eddy current measurements during the time the thermocouple readings were taken. A histogram of the deviations is shown in Figure 5. The 3-sigma variation was found to be $\pm 16°C$. We attribute the major part of this spread to arise from true variation of the temperature of the aluminum under test. Fluctuations in transport speed produced different degrees of cooling of the aluminum before it reached the eddy current sensor. This was detected by sequences of thermocouple measurements and also on recordings of data from the infrared sensor. We expect that future experiments with improved temperature control will reduce this limitation on our ability to obtain a measure of the ultimate precision of the eddy current system.
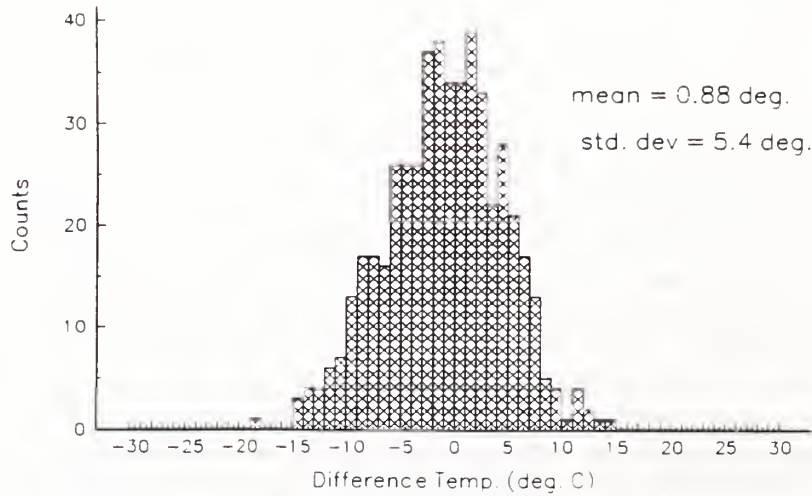
Fig. 5. Histogram of deviations of eddy current temperature readings from average thermocouple values. The 3-sigma value is $\pm 16°C$.

REFERENCES

1. A. H. Kahn and M. L. Mester, "Through-Transmission Impedance Measurements on Moving Metallic Sheets," Review of Progress in Quantitative Nondestructive Evaluation, Vol. 11, p. 249. Edited by D. O. Thompson and D. E. Chimenti, Plenum Press, New York, 1992.

2. M. Gvishi, A. H. Kahn, and M. L. Mester, "Eddy Current Testing of Carbon-Carbon Composites," Review of Progress in Quantitative Nondestructive Evaluation, Vol. 11, p. 289. Edited by D. O. Thompson and D. E. Chimenti, Plenum Press, New York, 1992.

3. J. M. Ziman, "Electrons and Phonons, The Theory of Transport Phenomena in Solids," Oxford, see p. 337, et seq., 1960.

4. J. T. Milek and S. J. Welles, "Electrical Resistivity of Aluminum and Chemical Composition and Electrical Resistivity of Aluminum Alloys," Properties of Aluminum and Aluminum Alloys, Y. S. Touloukian, and C. Y. Ho, eds., Thermophysical Properties Research Center, Purdue University, West Lafayette, IN, see pp. 516-522, 1973.

Fluorescence and Optical Monitoring of Polymer Processing

A. J. Bur (301-975-6748) and F. W. Wang
Polymers Division, Materials Science and Engineering Laboratry

The objective of this program is to develop in-line[1] measurement technology based on optical measurement methods to monitor important polymer processing parameters. The major optical method employed involves the detection of fluorescence spectra from fluorescent dyes which have been doped into the processed polymer material. The character of the fluorescence, i.e. its intensity, polarization, and wavelength distribution, yields information about the state of the polymer matrix. We have concentrated on developing concepts and methods to measure shear and extension stress, shear and extension strain rate, non-Newtonian viscosity, temperature, morphology and the onset of thermodynamic transitions.

The measurement goals of this program were established after extensive exchange of information with industry to determine measurement needs which can not be fulfilled using today's technology. Interaction with the polymer processing industry was formalized with the establishment of an NIST/industry consortium, New Measurement Technology for Polymer Processing. This consortium, which is centered at NIST, was initiated on June 1, 1992. Membership in the consortium remains open until November 30, 1992.

Over the past year our specific objectives have been to initiate the consortium research program, to measure fluorescence anisotropy of rod-like probes under both shear and extensional stresses, to design an extensional flow apparatus, to develop a model for in-situ measurement of extensional strain rate, and to collaborate with Drexel University employing optical and ultrasonics measurements to monitor polymer injection molding. Three significant achievements are summarized:

o The establishment of an NIST/industry consortium whose purpose is to develop real-time measurement technology based on optical and fluorescence methods to monitor important processing parameters;

o The fluorescence anisotropy of rod-like probes doped into a polymer melt matrix was measured as a function of shear and extensional stress. We observed that the anisotropy was insensitive to applied shear stress, but displayed significant change with the application of extensional stress. Thus, these probes can be used to monitor the presence of extensional flow fields in the presence of overlapping shear flow;

o In collaboration with Drexel University, an injection mold machine was instrumented with both ultrasonic and optical probes. Mold filling, crystallization and polymer solidification are being studied with these sensors.

---

[1] In the polymer processing industry, a distinction is made between in-line and on-line measurements. In-line refers to measurements made on the main process stream of flowing polymer material. On-line refers to measurements made on a small amount of material which has been diverted from the main stream and directed to the specimen chamber of an auxiliary instrument. In some cases, the diverted material is returned to the main stream; in other cases, it is discarded or recycled.

New Measurement Technology for Polymer Processing Consortium. This consortium is an outgrowth of an NIST/industry workshop which was held at NIST in December, 1990 [1]. The objectives of the workshop were: (a) to seek industry responses to the question: what in-line, real-time measurements do you need to make during polymer processing but are unable to do so because the measurement technology does not exist? and (b) to put together a collaborative NIST/Industry research program for the development of new measurement technology. Processors identified their measurement problems by describing various processing operations. Workshop discussions yielded a consensus of the following measurement needs: (a) in-line rheological measurements; (b) improved in-line temperature measurements; and (c) in-line and on-line measurements of polymer morphology. The direct interaction with industry at this workshop provided the framework for defining the consortium research program which is dedicated to the development of new in-line measurement technology for polymer processing based on optical and fluorescence methods. The consortium research program will extend over a period of four years during which time rheology and temperature measurement systems and concepts will be developed.

Fluorescence Anisotropy Measurements. This measurement involves the use of polarized light to determine the anisotropy of a fluorescent dye molecule which has been doped into a polymer matrix at very low concentrations. In previous work we used anthracene tagged polybutadiene as a fluorescent probe doped into a polybutadiene matrix. For this probe, anisotropy was found to decrease with increasing shear stress; a model to describe this behavior was developed [2,3]. The difference between the shear and extensional stress effects was examined by developing a model for the relationship between anisotropy, molecular orientation factors, shear stress and extensional stress. An essential requirement for anisotropy sensitivity to shear stress is that the probe molecule engage in the entanglement network of the matrix polymer, i.e., it must be macromolecular in size. Thus, under shear stress the anthracene tagged polybutadiene probe showed significant change with shear stress, but small fluorescent probe molecules, which are unable to engage in the molecular entanglement network of the matrix, are insensitive to shear stress.

For extension, we have observed that the entanglement requirement does not apply. This is probably because large orientations are possible under extension stress whereas only limited weak orientation occurs under shear stress [2,3]. Small rod-like fluorescent molecules, such as anthracene and diphenyl hexatriene, which associate their long axis with the polymer main chain extension, display fluorescence anisotropy change with applied extension stress, but show no significant change with shear stress. These observations were carried out using cross-linked polybutadiene. They demonstrate that the rod-like probes can be used to detect the presence of extensional stress in a mixture of extension and shear stress fields. Future extension experiments will be done using polymer melt (uncross-linked) in flow. To do this, we designed an extension flow apparatus with which the flow can be controlled with a constant strain rate.

Optical and Ultrasonics Monitoring of Injection Molding. The objective of this program is to develop new measurement methods for monitoring polymer injection molding processing. Ultrasonics and optical measurements are being employed to measure in real-time resin flow front velocity, mold filling time, resin temperature at the injection nozzle, onset of resin solidification in the mold, part shrinkage upon solidification and cooling, and resin modulus. We have made considerable progress with several of these measurements, e.g. mold filling time and solidification time. The data present a view of resin state changes in the mold cavity during the most critical phase of the mold cycle.

REFERENCES

1. A. J. Bur, P. Handa and C. Grudzien, "Workshop on New Measurement Technology for Polymer Processing," NIST J. Res. **6**, 503 (1991).

2. A. J. Bur, R. E. Lowry, S. C. Roth, C. L. Thomas, and F. W. Wang, "Observations of Shear Induced Molecular Orientation in a Polymer Melt Using Fluorescence Anisotropy Measurements," Macromolecules **24**, 3715 (1991).

3. A. J. Bur, R. E. Lowry, S. C. Roth, C. L. Thomas, and F. W. Wang, "Fluorescence Anisotropy Measurements on a Polymer Melt as a Function of Applied Shear Stress," Macromolecules **25**, 3503 (1992).

Electroacoustic Measurements in Dense Ceramic Slurries

S. G. Malghan (301-975-6101) and V. A. Hackley
Ceramics Division, Materials Science and Engineering Laboratory

R. Mountain (301-975-2484)
Thermophysics Division, Chemical Science and Technology

Colloidal processing of powders for advanced structural ceramics requires stringent control of particle dispersion in a liquid medium. The tendency to form agglomerates, especially in dense systems where interparticle distances are minimal and interactions are strong, will lead to undesirable properties in the green body (e.g., nonuniform sintering rates, microstructural defects, etc.). Dispersion in aqueous solution, the most common method, is dependent primarily on the electrochemical properties of the powder-solution interface, and can be monitored using techniques that are sensitive to the shear-plane or zeta potential. Standard methods for the determination of zeta potential depend on optical scattering and are therefore incompatible with dense, optically opaque slurries. In this case, electroacoustic methods have been successfully applied [1, 2], although many of the interrelationships between such measurements and the physicochemical parameters of dense suspensions have yet to be firmly established. Additionally, the electroacoustic probe geometry and robust design allow for the development of systems for on-line analysis and intelligent processing. Our objectives are the establishment of the measurement of sample parameters in their relationships and development of an on-line system in collaboration with Matec Applied Sciences, Inc.

Our work focuses on electrokinetic sonic amplitude (ESA) measurements in silicon nitride powder suspensions. Essentially, this technique measures the coherent ultrasonic response of charged colloids to an applied alternating electric field [3]. ESA is the measured pressure amplitude of the ultrasonic wave per unit applied electric field (*P/E*), and depends on several parameters according to the relation

$$ESA(\omega) = \frac{P}{E} = c\ \Delta\rho\ \phi\ f_G\ \mu(\omega)$$

Here ω is frequency, c is sound velocity, $\Delta\rho$ is the density difference between particle and medium, ϕ is the particle volume fraction and f_G is a factor that depends on electrode geometry. The key variable is the dynamic (high-frequency) particle mobility $\mu(\omega)$, which is related to the zeta potential and powder electrochemical dispersion properties.

Standard procedures for sample preparation and electrokinetic sonic amplitude analysis of silicon nitride powders have been established within our laboratory. This was critical to facilitate investigation of the various effects of instrumental, experimental and powder parameters with a high degree of confidence in such results. We have also examined the reproducibility of the ESA measurement, in particular with reference to the performance of acidimetric-alkalimetric titrations and the determination of the powder's isoelectric point (pH_{iep}) (the pH at which the particles are electrically neutral). The pH_{iep} is the key surface chemical characterization parameter for a powder. Results indicate that titration curves are highly reproducible when taken over the course of several days; however, we find that in some of the powders, slow aging processes occur which lead to a small systematic shift in the pH_{iep}. This must be taken into consideration for process control and in the design of experiments and interpretation of results.

A parametric analysis of the ESA measurement yielded results for the volume fraction dependence, effect of background electrolytes and path-dependent effects of the mode of titration during analysis. Linear behavior was observed for ESA as a function of the particle volume fraction up to 10% solids. Analysis was performed on samples up to 30% volume fraction. It was also found that background electrolytes may contribute significantly to the apparent powder ESA signal amplitude and phase angle, particularly at lower particle concentrations and near pH_{iep}. It is possible to subtract the background signal if it is measured separately as a function of pH. It is also possible to select an electrolyte pair that gives an insignificant background signal ($NaNO_3$ is an example). Finally, we find that the path-dependency of a titration may affect the measured pH-dependent behavior of the ESA signal under certain conditions. To this end, we have documented various methods for performance of acid-base titrations.

A critical study was completed in which several commercial silicon nitride powders were characterized by ESA, and then treated with an aqueous soxhlet extraction surface-cleaning procedure. Results (Figure 1) show a linear relationship between the oxide layer thickness measured by Auger electron spectroscopy and pH_{iep} determined from ESA analysis for these powders, irrespective of particle size or the chemical process by which they were produced. This indicates a fundamentally important correlation between oxide formation on the nitride surface and dispersion properties. The results of this study will be included in a future publication which we are currently preparing.

Correlation of electrophoretic mobility and ESA measurements is considered a top priority for fiscal year 1993. It is essential to relate ESA to more established methods for determining zeta potential in dilute systems. We expect continued cooperation with Matec Applied Sciences on the development of an on-line electroacoustic sensing device. Work will continue on the parametric investigation of the ESA measurement, focussing on powder parameters such as particle size and size distribution. Additional studies have been initiated, including powder-polymer interactions in mixed systems containing binders
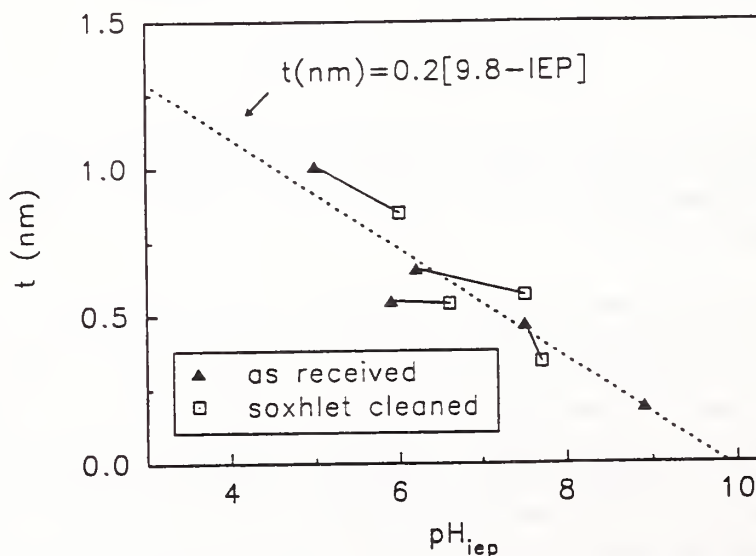

Fig. 1. Surface oxide layer thickness (t) as function of the isolectric point (pH_{iep}) determined from electroacoustic measurements of silicon nitride suspensions.

32

and dispersants. This correlation of the measurements will be incorporated in a quantative model currently being developed. This model will describe the operation of the ESA system as part of a process monitoring operation.

Work on the development of simple models to connect ESA measurements with the properties of a high volume fraction slurry has started. A cell model formulation appears to be a useful approach [4, 5]. The sensitivity of measurements to important characteristics of the slurry, such as degree of aggregation, polydispersity and density gradations, will be examined within this model framework.

REFERENCES

1.   V. A. Hackley, R. S. Premachandran and S. G. Malghan, "Electrokinetic sonic analysis of silicon nitride suspensions," submitted for publication in Ceramic Transactions (1992).

2.   R. W. O'Brien, B. R. Midmore, A. Lamb and R. J. Hunter, "Electroacoustic studies of moderately concentrated colloidal suspensions," Disc. Faraday Soc., 90, 301 (1990).

3.   R. W. O'Brien, "The electroacoustic equations for a colloidal suspension," J. Fluid Mech., 212, 81 (1990).

4.   B. J. Marlow, D. Fairhurst and H. P. Pendse, "Colloid vibration potential and the electrokinetic characterization of concentrated colloids," Langmuir, 4, 611 (1988).

5.   Discussion of [2], pp. 359-363.

Development of Electromagnetic Probes for Intelligent Processing of Dielectric Materials

A. V. Clark (303-497-3159) and S. R. Schaps
Materials Reliability Division, Materials Science and Engineering Laboratory

J. Baker-Jarvis (303-497-5621) and R. G. Geyer
Electromagnetic Fields Division, Materials Science and Engineering Laboratory

B. A. Auld, Stanford University

Electromagnetic probes are useful for characterizing the dielectric properties of materials and in the intelligent processing of materials. As an example, consider the electronic industry, which produces dielectric substrates for electronic packaging of MMIC, stripline, and semiconductor devices. Here a high degree of homogeneity of dielectric properties (typically $\pm 2\%$) is desired over the microwave spectrum. The Electromagnetic Fields Division and the Materials Reliability Division, are collaborating on research to explore the potential of electromagnetic probes for these and other practical applications to the processing of dielectric materials. Work is proceeding to model the behavior of the probes, to perform laboratory experiments to characterize the probes, and to demonstrate their practical utility. The probes used in this research can operate with a clearance between probe and specimen (lift-off) to inspect material in a process control mode. Since probe response is sensitive to lift-off, we are currently investigating techniques for separating the effects of lift-off and complex permittivity. Two types of probes are being studied: 1) coaxial probes operating in the 100 MHz to 10 GHz frequency range and 2) planar electrode arrays operating in the 100 kHz range.

Coaxial Probes. The coaxial probe consists of a coaxial line with an open-circuit termination [1, 2]. Three probes were developed: 3.5 mm, 7 mm, and 35 mm diameter. Theory and numerical modeling for these probes, with lift-off, were completed [3]. Calibration techniques, which consist of measuring an open-circuit, a short-circuit, and a liquid such as water, were developed for the probes.

In industrial applications, such as for rolling stock on an assembly line, it is usually necessary to measure quantities of interest in a noncontacting manner. The theoretical model of the open-ended probe with lift-off was developed with this constraint in mind. The model allows prediction of the reflection coefficient as a function of lift-off over the sample under test for both samples of semi-infinite extent and samples terminated by a short-circuit. The variation of the reflection coefficient $|S_{11}|$ over a dielectric material depends both on probe size and frequency of operation as shown in Figure 1. It is seen that for large lift-off, (d > b-a) where b and a are the outer and inner radii of coaxial line, the probe is essentially an open-circuit. The degree to which the electromagnetic fields penetrate into the material under test is determined by the probe size and frequency. At low frequencies the magnitude of the reflection coefficient is close to 1. It is seen that larger probes interact more strongly with the material under test through larger penetration depths. However, large probes yield lesser spatial resolution.

In the last year a number of substrate materials were obtained from manufacturers such as Coors, Rogers Corporation, and Hewlett Packard. The open-ended coaxial probe was used for substrate measurement on materials obtained from these companies, with and without lift-off.

Array Probes. Figure 2 shows one prototype array probe currently under investigation, designed for defect detection. Another version of this 4-electrode array structure, with the array elements connected
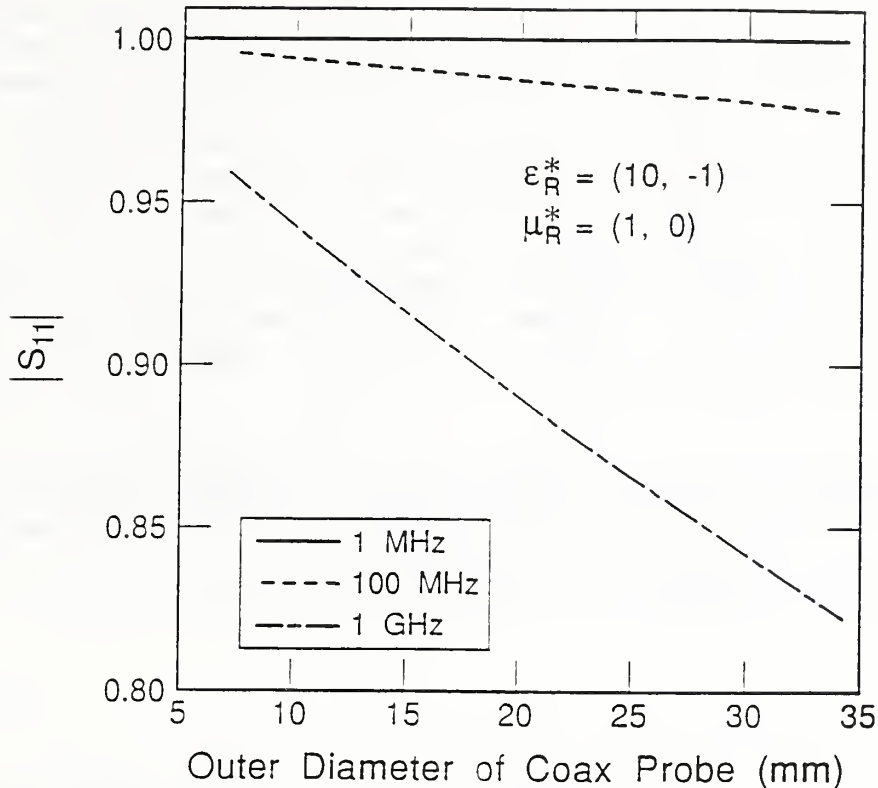
Fig. 1. Magnitude of the reflection coefficient as a function of probe outer diameter at various frequencies of operation.

to a bridge-type circuit arrangement, has been used for material characterization. A theory was developed for the change in probe admittance due to small defects [4-6]. Experiments were carried out on large well-characterized defects (volume of the order of 10^3 mm^3) using the probe shown in Figure 2; the results show the same features predicted by theory. The theory predicts that for smaller probes (which concentrate the probe electric field), sensitivity to defects is enhanced. The experiments also showed how various noise sources could be suppressed. This combined analytical/experimental approach predicts that defects of interest in dielectric substrates should give probe signals about two orders of magnitude larger than the noise level.

Practical Applications. For production of high-quality dielectric substrates, green state material is rolled to obtain the desired densification and thickness. These parameters are typically measured off-line for quality assurance. It would be desirable to characterize densification and thickness on-line on rolled stock prior to the highly value-added steps of sintering. Measurement of capacitance can provide a means to do this, using either the coaxial or array type of probes. For example, the capacitance of a simple parallel plate capacitor depends on material thickness and dielectric constant, ϵ.

Green state material consists of several phases: powder, binder, and voids (entrapped air). "Mixing rules" relate ϵ of the material to the dielectric constants of the phases; the contribution of each phase depends upon its volume fraction. Also, the density of the material obeys a "mixing rule" relation;

35

the density equals the weighted sum $\Sigma n_i \rho_i$ where n_i is volume fraction of the ith constituent and ρ_i is the corresponding density. From relations such as these, it can be shown that changes in densification (and hence in volume fractions) result in changes in ϵ, and hence in probe capacitance. Likewise, changes in thickness produce changes in capacitance (4-6). This leads to the following simple inspection concept. The permissible range of thickness and densification variations are specified; typically, the percent variation in thickness and densification is no more than $\pm 0.5\%$ about the desired values. The effective change in probe capacitance due to these variations can be estimated by the "mixing rule" concept above. The capacitance with "good" samples could be measured and used as a baseline (reference). Any samples resulting in capacitance changes outside the allowable variations are, therefore, "unacceptable". Research on proof-of-concept is in progress. Actual production samples were obtained from a manufacturer of high-quality dielectric substrates. Initial measurements were made with no probe liftoff. These indicate that all samples are "acceptable", i.e., the variation in probe capacitance with different samples is within the "allowable" bounds.

Typical defects in dielectric substrates after firing are through-cracks having volumes of the order of 1 mm³. Such defects are unacceptable for electronic packaging applications. Defects can be detected off-line with e.g. dye penetrant. A rapid, noncontact inspection in principle can be done with electromagnetic probes, provided that a sufficient signal-to-noise ratio can be achieved. Modeling of the probe prototype in Fig. 2 indicates that sufficient sensitivity is possible.
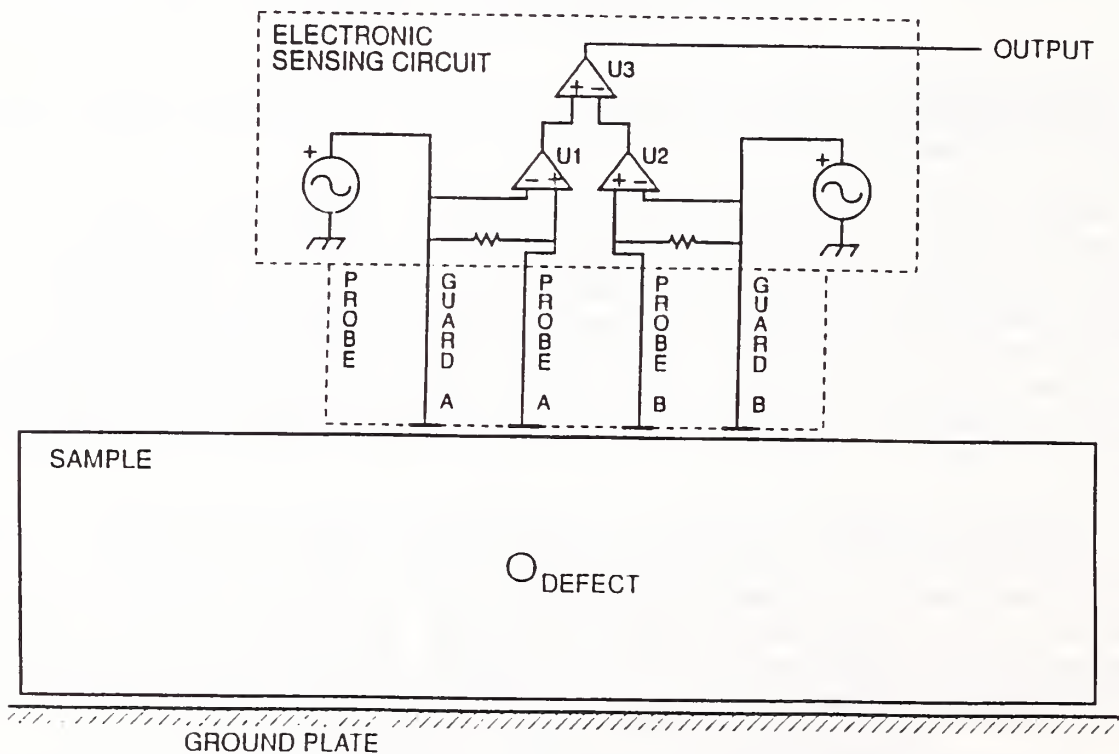

Fig. 2. Capacitive probe and electronics used for proof-of-concept experiments of defect detection.

REFERENCES

1. J. R. Baker-Jarvis, M. D. Janezic, J. H. Grosvenor, Jr., R. G. Geyer, "Transmission\Reflection and Short-Circuit Line Methods for Measuring Permittivity and Permeability," NIST Technical Note **1355** (1992).

2. R. G. Geyer, "Dielectric Characterization and Reference Materials," NIST Technical Note **1338**, 1990.

3. J. R. Baker-Jarvis and R. G. Geyer, "Nondestructive Testing with an Open-ended Coaxial Probe with Lift-off," URSI Digest, p. 282, Boulder, CO., 1992.

4. M. Gimple and B. A. Auld, "Variable Geometry Capacitive Probe for Multipurpose Sensing," Res. Nondestr. Eval. **1**, 111 (1989).

5. V. K. Tewary, P. R. Heyliger, and A. V. Clark, "Theory of Capacitive Probe Method for Noncontact Characterization of Dielectric Properties of Materials," J. Mater. Res. **6**, 629 (1991).

6. B. A. Auld, "Capacitive NDE and Material Characterization Probes," Final Report to NIST, Service Contract 43NANB017582, June, 1991.

PUBLICATIONS

1. J. R. Baker-Jarvis and Richard G. Geyer, "Nondestructive Testing with an Open-ended Coaxial Probe with Lift-off," URSI Digest, p. 282, Boulder, CO., 1992.

2. J. R. Baker-Jarvis and R. Stafford, "Analysis of an Open-Circuit Sample Holder for Dielectric and Magnetic Measurements," paper through review process for NIST-IR, 1992.

3. J. R. Baker-Jarvis, M. D. Janezic, and R. G. Geyer, "Theory of a coaxial probe with lift-off for nondestructive testing," in review for IEEE Transactions on Instrumentation and Measurement, 1992.

Ultrasonic Measurements of Subsurface Damage for Ceramics Processing Control

G. V. Blessing (301-975-6627), N. N. Hsu, and J. A. Slotwinski
Automated Production Technology Division, Manufacturing Engineering Laboratory

The objective of this research project is to evaluate the capability of ultrasonic techniques to nondestructively assess surface and subsurface damage in ceramics caused by surface grinding. In particular, ultrasonic wave propagation techniques using noncontact sensors are pursued for their potential to sense subsurface structure and possibly to correlate this structure with surface conditions. The capability of these sensors for in-process application lends emphasis to their development.

Motivation for this work stems from the manufacturing industry's crucial interest in the surface condition of ceramic products. Product strength is substantially influenced by surface layer properties. It is important to evaluate and minimize near-surface grinding damage sites which will influence crack growth under service stress. The depth of this damage may extend from tens to hundreds of micrometers depending on the grinding speed, rate of material removal, grit size and other factors. While rapid grinding with a large grit may be the most efficient for part production, a balance must be reached with the residual material damage that may accrue.

Previous studies on ground quartz samples imply that high frequency elastic waves may be sensitive to subsurface structure. Compressional wave tone bursts at ultrasonic frequencies were coupled through a water medium and directed normal to the ground surfaces. Structure in the echoes from the quartz-water interface was observed to be very different for two samples subjected to different grinding conditions. An understanding of this apparent sensitivity to subsurface structure is a principal part of this investigation.

Two types of ultrasonic wave interrogations are proposed for use with a liquid coupling medium: near-normal incidence compressional waves and refracted surface waves. Compressional waves have their material displacement vector parallel to the direction of wave propagation, thereby imposing an oscillating pressure normal to the interface. Possible mechanisms by which this wave type may be sensitive to subsurface structure are via (a) compliance changes in the material, and (b) phase interference between the surface reflections and subsurface micro-crack reflections occurring within some region of "penetration depth" for the compressional waves. Surface waves travelling parallel to the interface in the material will be sensitive to cracks and pores whose plane of orientation is normal to that propagation direction. During propagation, this wave type radiates or "leaks" back into the liquid at a critical angle obeying Snell's law of refraction for the wave speeds in the liquid and solid media.

Silicon Nitride (Si_3N_4) samples were provided by C. Evans of the Precision Engineering Division and S. Jahanmir of the Ceramics Division. Some samples have an extensive evaluation history by materials researchers, giving us a known basis for comparison. They were ground in one direction, and half the surface subsequently polished to remove the damaged layer in a taper from the ground surface down to the undamaged region, as determined microscopically. In order to estimate the expected surface-mode sound speeds and the critical angles that pertain, bulk speed measurements of compressional and shear waves were made. These values were respectively 10.6 and 5.9 mm/μs, assuring that the critical angles for all surface modes would be less than 20° from the normal. These elastic wave speeds were needed to model the wave interaction at the water/ceramic interface by means of a Green's function
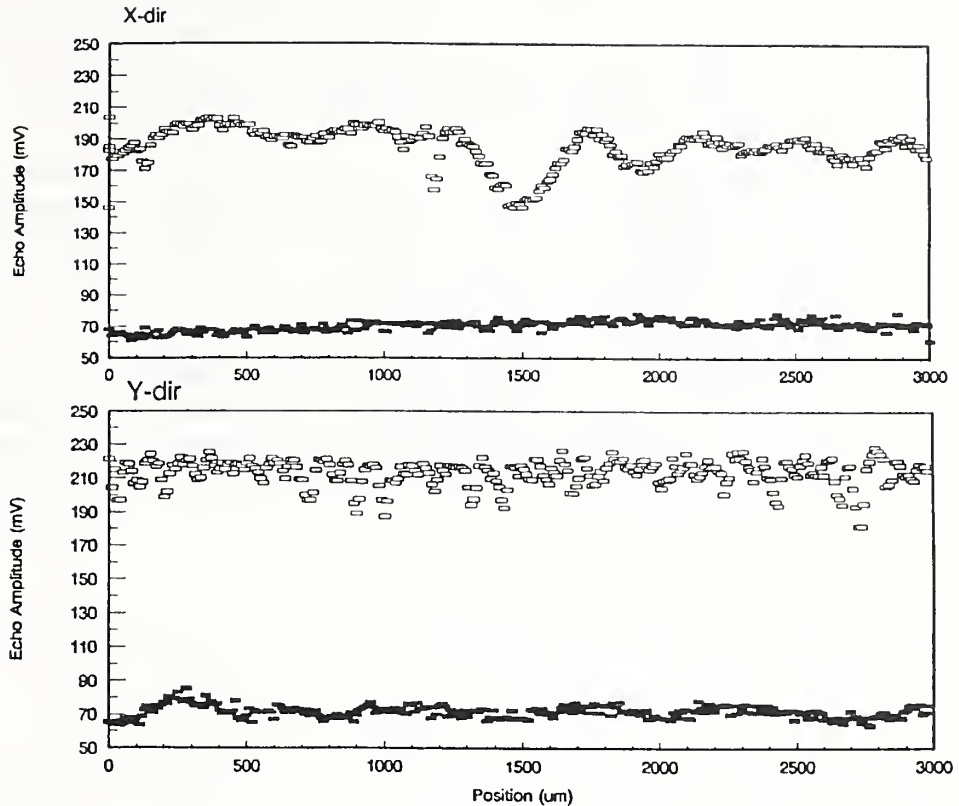
Fig. 1. Echo amplitude recordings of ultrasonic scans taken parallel (X-dir) and perpendicular (Y-dir) to the grinding grooves of a ceramic sample. The top traces of each scan direction are recordings of the echoes from the water/sample interface. The lower traces are recordings of leaky-wave echoes taken with the sensor de-focused.

formulation. A point source and a detector equidistant 1.0 mm from the solid surface and separated by 4.0 mm were assumed. A convolution of an incident wave form, simulating a symmetrically damped one-and-a-half cycle sinusoid, with the Green's function for the ceramic medium was performed. The results predicted a shear "head" wave preceding and phase-reversed relative to the normal-incident direct-reflected wave.

Experimental results were obtained using a spherical-focus 50 MHz transducer attached to a silicon buffer rod, with a 0.8 F-number lens ground at the other end. The sensor was positioned in its defocused near-field region relative to a Si_3N_4 sample surface. We observed a phase-reversed wave form, preceding the normal-incidence water echo, under experimental conditions comparable to the model configuration except for the point-sensor assumption. Future work calls for improved modeling of the experimental situation by assuming rings of point sources (and detectors) with radii extending from zero to the lens aperture value.

An X-Y micro-positioning translation stage with 0.1 μm resolution was assembled and interfaced to a PC controller. Software was developed for linear and raster scans, with graphic displays of echo-amplitude and transit-time data. A basic statistical analysis capability for specified scans is a part of the

software. Figure 1 represents typical ultrasonic scans taken parallel (X-dir) and perpendicular (Y-dir) to the grinding grooves of a sample. The top traces for each scan direction are recordings of the detected echo amplitude taken with the sensor focused at the sample surface and normal to it. Whereas stylus measurements revealed that the average surface roughness value parallel to the grinding was one-half that perpendicular to it, a more variable structure (of lesser average amplitude) is observed for the parallel scan. The lower traces in Fig. 1, which are recordings of the leaky-wave echoes taken with the sensor de-focused, also reveal a somewhat distinctive structure from each other. Repeated scans at random sample locations produced this consistent behavior. We cannot yet confidently explain these results, but conjecture that we may be sensing subsurface damage which is directional in nature.

We note that the tightly focused sensor used here produces a narrow focal region of incident compressional waves yielding good lateral resolution, but is not an optimum design for surface wave generation and detection. Custom sensors are being designed, with separate transmit and receive elements for operation in a pitch-catch mode to maximize specific surface modes and minimize normal-incidence rays.

Laser Ultrasonics for Metals

W. L. Johnson (301-975-6144) and J. B. Spicer
Metallurgy Division, Materials Science and Engineering Laboratory

The objective of this effort is to develop laser-ultrasonic techniques for performing ultrasonic measurements on steel alloys at elevated temperatures which are still below the alloy melting point. Many processes for hot shaping of alloys require that the bulk temperature exceed a threshold value before processing can begin. Ultrasonic testing which correlates ultrasonic time-of-flight measurements with the temperature of the alloy may be performed to ensure that this threshold is achieved during heating or reheating. Using laser ultrasonic techniques allows these measurements to be accomplished with minimum intrusion into the process. It was first necessary to outline two areas of investigation. The first is a study of the laser source in relation to the steel temperature so that optimization of the source may be achieved. The second is the development of laser ultrasonic apparatus capable of making ultrasonic time-of-flight measurements from the rough surfaces that will be encountered in industrial processing environments.

The study of the laser source at elevated temperatures consisted of laboratory tests in which several different stainless steel alloys were tested with laser generated ultrasound at temperatures ranging from 300 K to over 1273 K. The alloys were tested by exciting ultrasound in a sample with a pulsed Nd:YAG laser and detecting the epicentral ultrasonic displacements on the opposite side of the sample with a Michelson-type interferometer. By maintaining the laser source fluence in the thermoelastic regime for these tests, displacements at both the longitudinal and shear wave times-of-arrival could be determined easily and reproducibly. Some of the waveforms detected in an AISI 303 stainless steel, shown in Fig. 1, are seen to change as a function of the sample temperature. Determinations of both the longitudinal and shear wavespeeds were made from these waveforms and are plotted as a function of
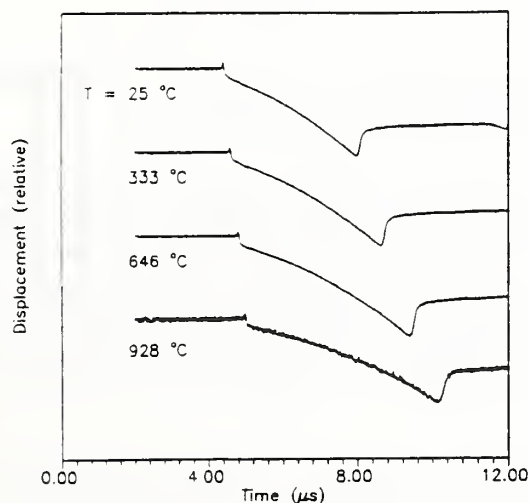

Fig. 1. Thermoelastic, displacement waveforms in AISI 303 stainless steel at different sample temperatures. The scale of the ordinate axis is the same for all waveforms.

sample temperature in Fig. 2. Previous results for the longitudinal wavespeed in AISI 304 as a function of temperature, obtained using contacting transducers [1], are consistent with the results presented here. Our results for the shear wavespeed are the first known reported measurements at elevated temperature. The shear wavespeed changes as a function of temperature indicate a greater percentage change than for the longitudinal wavespeed.
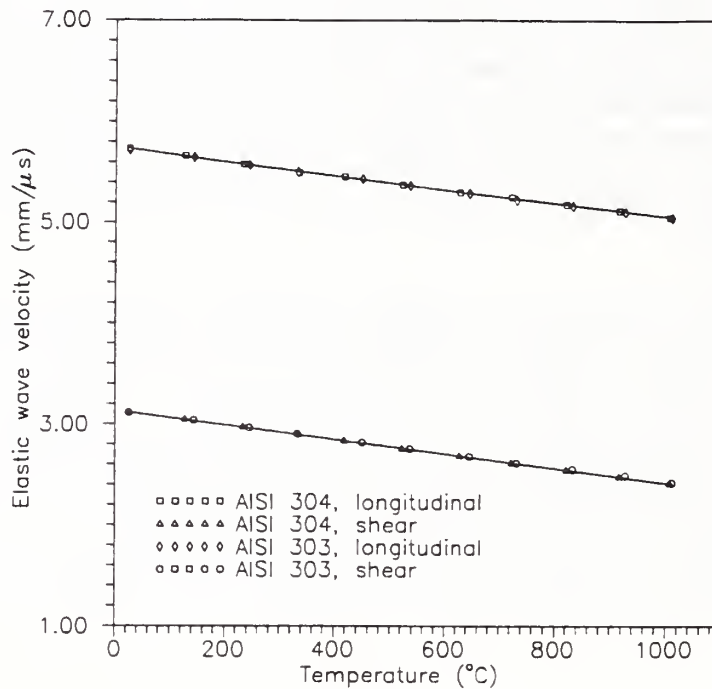

Fig. 2. Wave velocities in AISI 303 and 304 as a function of sample temperature. The solid curves represent second-degree polynomial equations fitted to the data.

Along with the velocity changes observed with increasing temperature, the displacement amplitudes in the AISI 303 and 304 alloys also increased with the sample temperature until the temperature approached 1100 K. Above this temperature the displacement amplitudes decreased markedly with increasing temperature. Concurrent modeling efforts using dynamic thermoelasticity theory [2] indicate that the initial increases in displacement cannot be attributed to the changes in elastic or thermal properties of the material but are most likely a result of increased absorption of the source laser pulse. The reduction in displacement above 1100 K is not understood yet and is being investigated further.

The second part of the program addressed methods for implementing laser ultrasonics in an industrial environment. Various designs for acousto-optically stabilized Fabry-Perot interferometers were analyzed, constructed and tested to detect laser ultrasonic disturbances from the type of rough surfaces that might be encountered on a process line. The use of Fabry-Perot interferometers for laser ultrasonics is well established [3] and is seen to be the most direct method for making laser ultrasonic measurements in industrial processes. Current plans include using one of the designs in a long-pulsed, high-power,

Fabry-Perot interferometer for detection of ultrasound at rough, oxidized surfaces. Efforts currently are directed toward fabrication of a suitable Fabry-Perot system.

REFERENCES

1. H. N. G. Wadley, S. J. Norton, F. Mauer and B. Droney, "Ultrasonic measurement of internal temperature distribution," Phil. Trans. Royal Soc. London, A **320**, 341 (1986).

2. J. B. Spicer, "Laser ultrasonics in finite structures: Comprehensive modeling with supporting experiment," Ph.D. dissertation, The Johns Hopkins University, 1991.

3. J. P. Monchalin, "Optical detection of ultrasound at a distance using a confocal Fabry-Perot interferometer," Appl. Phys. Lett. **47**, 1, 14 (1985).

Depth of Case Hardening

A. H. Kahn (301-975-6146) and L. C. Phillips
Metallurgy Division, Materials Science and Engineering Laboratory

D. Lu, Student Associate, Johns Hopkins University
K. White, Guest Worker, Saginaw Division, General Motors Corporation

This cooperative effort of NIST and the General Motors Corporation has the objective of assessing the applicability of eddy current methods for the determination of the depth of case hardening in steel drive axles treated by induction heating, followed by quenching. In the first year the objective was to perform measurements on several hundred specimens prepared to have a wide range of nominal case hardening depths. The measurements were completed and the results will now be compared with the results of destructive testing on the same axle samples.

In the range of samples available, the case hardening process alters the microstructure of the axle to a depth of 3 to 6 millimeters, depending upon process parameters. Concurrent with the microstructure changes are changes in the electrical conductivity and the magnetic permeability of the axle in the region which was hardened. Eddy current measurements are sensitive to the electrical and magnetic properties of the test material. In addition, the electromagnetic skin effect may be used to advantage. Low frequency magnetic fields penetrate deeply into the test material; high frequency magnetic fields penetrate only a short distance. By examining eddy current measurements over a range of frequencies, one may distinguish variations with depth of the magnetic and electrical properties of the treated materials. Correlation of the eddy current detection of these property changes with hardness must finally be verified by destructive testing of the examined samples. Typical curves of eddy current dissipation as a function of frequency for several different case depths are shown in Figure 1.
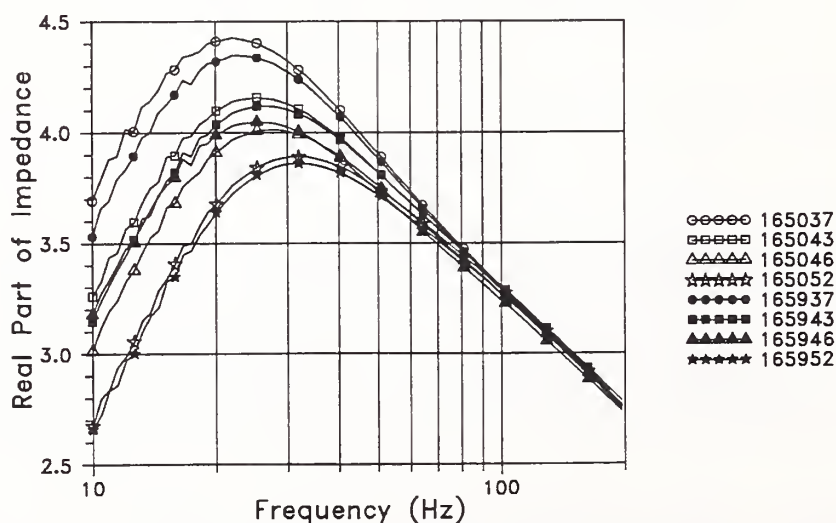

Fig. 1. Plot of the real part of the sensor transfer impedance vs. frequency for a group of case hardened drive axles. The real part of the impedance is proportional to the eddy current dissipation of energy. The legend identifies test samples; the last two digits represent the case depth as 3.7 mm, 4.3 mm, etc. Note the pairing of the curves for samples of the same nominal case depth.

Sensor coils were constructed for testing the drive axles, which were milled shafts approximately 30 cm long and 2.5 cm in diameter. The test coils and apparatus were similar to that used for extruded rods, as described below[1]. The coil system consisted of a primary solenoid 20 cm long and 6.4 cm in diameter. The secondary coil lies centered within the primary and was tightly wound to interrogate only a small part of the test sample. Measurements were made from 10 Hz to 200 Hz. A series of 360 observations was analyzed statistically. It was found that the characteristic of the eddy current dissipation vs. frequency curves most directly related to nominal case depth was the magnitude of the peak dissipation minus the dissipation at 10 Hz. The 360 observations represented 2 heats, 3 nominal depths, 3 locations on the shafts, 2 samples each, and 10 replications for each location. It was found that the overall standard deviation of the dissipation difference was 0.161, while the standard deviation of this quantity for repeatability on the same sample was 0.012. (In terms of variance of the expected case depth, this is equivalent to 0.48 mm for the samples overall and 0.036 mm for the variance associated with repeatability.) The low variance on repetition suggests that the measurement precision is adequate and that the variance over the different samples may be due to true differences in the hardness profiles of the samples. The final analysis will depend upon the destructive hardness testing which is now being performed.

REFERENCES

1.   A. H. Kahn, M. L. Mester, and H. N. G. Wadley, "Eddy Current Sensing of Deformation Processing," in Intelligent Processing of Materials, p. 393, edited by H. N. G. Wadley and W. E. Eckhart, Jr., The Minerals, Metals & Materials Society, 1990.

Nuclear Magnetic Resonance for Ceramics

Pu Sen Wang (301-975-6104)
Ceramics Division, Materials Science and Engineering Laboratory

In a ceramic green body, the binder distribution is a critical parameter that affects the final ceramic's mechanical, thermal, electrical properties, and reliability. An understanding of the interfacial reactions between the binder and ceramic powders under various processing parameters is essential to alleviate binder distribution related problems in ceramic processing technology. Efforts have been made to improve this understanding by nuclear magnetic resonance (NMR) imaging with gradient coils [1]. However, due to the line-broadening caused by nuclear dipolar interaction in solids, the development of NMR imaging for ceramic material application has been limited.

In "hard solids" like ceramics, the linewidth due to the nuclear dipolar interaction because of the restriction in atomic motion is often a few hundred times larger than that in the "mobile" samples. Consequently, line-narrowing and large field gradient are the two critical factors to a successful NMR imaging technique for solids. Previously, we reported the results of organic binder distribution in green body ceramics by NMR imaging utilizing a large field-gradient provided by the stray-field [2-4] together with a series of pulses for nuclear detection [5]. The development of an NMR imaging facility with gradient coils for the investigation of silicon nitride slurries in water before casting into green bodies was also reported [6].

Progress in 1992 includes: (1) A comparative study of binder homogeneity in green bodies; (2) Improvement of the gradient-coil micro-imaging facility for certain cases of solid imaging; and (3) Progress in developing an ^{27}Al stray-field imaging facility.

(1) Silicon nitride powders, with either polyethylene glycol (PEG) or polyvinyl alcohol (PVA) binders, were centrifugal-cast to cylindrical green bodies of 12 mm diameter and 10 mm thick, for a stray-field NMR imaging study. The % weight binder in these samples was $10.0\pm0.9\%$. Binder distribution was homogeneous in the PEG sample. However, in the PVA sample, the binder distribution was nonuniform in certain locations (Fig. 1). In this picture, white indicates a region with high binder concentration. It can be easily seen that the lower portion of the picture indicates a higher binder concentration than the upper portion. A stationary, nonspinning ^{1}H NMR spectroscopic study at 400.13 MHz shows that a sharp peak from the residual water was detected in the sample with PVA binder (Fig. 2). No such mobile protons from water were observed from the sample with PEG binder. This indicates that the green body cast with PVA binder under identical parameters as that of PEG has higher water content which maybe responsible for the inhomogeneous binder distribution in certain spots of the sample. Note that the strong broad peak in Fig. 2 is due to the solid protons in PVA.

(2) The high-resolution stray-field imaging for solids reported above utilizes the projection reconstruction technique. This technique requires long measuring time and complicated data handling. In contrast, the micro-imaging with gradient coils used for slurry mapping utilizes the nuclear spin echo technique [6]. One of the advantages of this is time-saving. In the past year, the multi-slice technique was developed for our facility. This technique provides the possibility for observing a number of slices (e.g. 4, 8, 16, 32,...) in a few minutes. It is almost impossible in this method to avoid a certain degree of overlapping of neighboring slices. However, the excitation sequence planned can minimize this overlapping. For example, in an eight-slice experiment, the order of excitation is 1-3-5-7-2-4-6-8. In

46

this manner, before slice #2 is excited, slice #1 and #3 have been relaxed. Nevertheless, this multi-slice spin echo NMR imaging technique is limited to materials with certain relaxation times. This, of course, is the price one has to pay for time-saving experiments. We have tested the green body samples by this imaging method and observed internal cracks in some ceramic pieces.

(3) Alumina (Al_2O_3) is another important ceramic material. In some ceramic composites, alumina is used as a reinforcement. The distribution of alumina in these systems provides valuable information for understanding the properties of these composites. An NMR imaging facility operating at the [27]Al frequency will provide us with the capability to obtain this information. We are continuing to pioneer the development of a high resolution solid NMR imaging technique at the [27]Al frequency utilizing the strong stray-field.

Compared to the ^{1}H imaging, ^{27}Al NMR imaging experiences the following difficulties:

o Lower Frequency: The NMR frequency can be calculated from $\gamma B/2\pi$ where B is magnetic field and γ is magnetogyric ratio. The magnetogyric ratios for ^{1}H and [27]Al are 26.7522×10^7 and 6.9762×10^7 rad s^{-1} T^{-1}, respectively. Equipment that resonants at 162.7 MHz for ^{1}H will resonate at 42.43 MHz for [27]Al. A suitable coil was constructed and is undergoing tests for phantom imaging.

o Low Sensitivity: The absolute sensitivity (relative sensitivity x natural abundant) of [27]Al nuclei is only 21% of that of [1]H. More scans are therefore required to obtain a picture of the same quality.

o Nuclear Quadrupole Broadening: The nuclear spin of ^{1}H is 1/2 but that of [27]Al is 5/2. How to overcome the quadrupole broadening in [27]Al is a challenge.

REFERENCES

1.   L. Garrido, J. L. Ackerman, W. A. Ellingson and J. D. Weyand, Ceram. Eng.
     Sci. Proc. 9, 1465 (1988).

2.   P. S. Wang, Intelligent Processing of Materials, NISTIR 4693, p. 48 (1991).

3.   P. S. Wang, D. B. Minor, and S. G. Malghan, presented in ASNT Spring Conference, Orlando,
     Florida, March 31 - April 1, 1992.

4.   P. S. Wang, D. B. Minor, and S. G. Malghan, in press, Journal of Materials Science (1992).

5.   J. H. Strange, Phil. Trans. R. Soc. Lond., A333, 427 (1990).

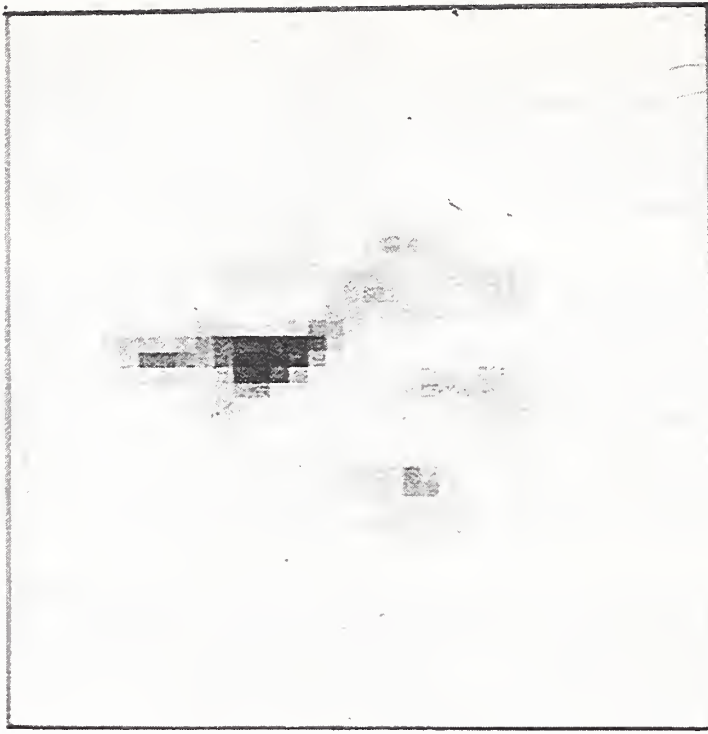6.   P. S. Wang, NDE Annual Report, NIST, 1990.

Fig. 1. A cross-sectional view of PVA distribution in a silicon nitride green body (12 mm diameter) containing 10% binder, as obtained by stray-field NMR imaging.
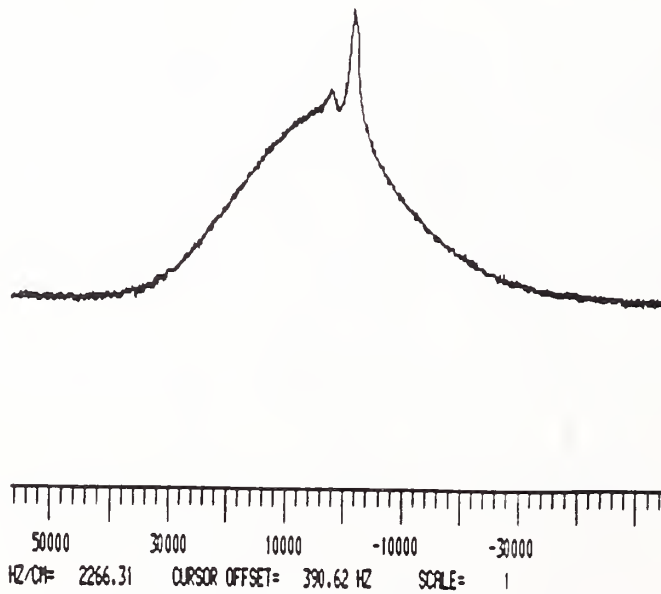


```
  50000      30000      10000      -10000     -30000
HZ/CM=  2266.31    CURSOR OFFSET=  390.62 HZ    SCALE=   1
```

Fig. 2. Proton NMR spectrum at 400.13 MHz of a silicon nitride green body containing 10% PVA binder.

NDE Standards and Methods for X-Ray Radioscopy

T. A. Siewert (303-497-3523), M. W. Austin, and D. L. Fitting
Materials Reliability Division, Materials Science and Engineering Laboratory

The objectives of this investigation are to develop, for radioscopy systems, measurement standards that are based on fundamental units and to develop the corresponding test methods. These developments have become increasingly important because the high cost of film and the delay in evaluating the images are causing many users to switch to imaging screen (radioscopy) systems. Unfortunately, these systems have slightly different capabilities from film, so that conventional image quality indicators and control procedures are not able to fully characterize the images from these systems.
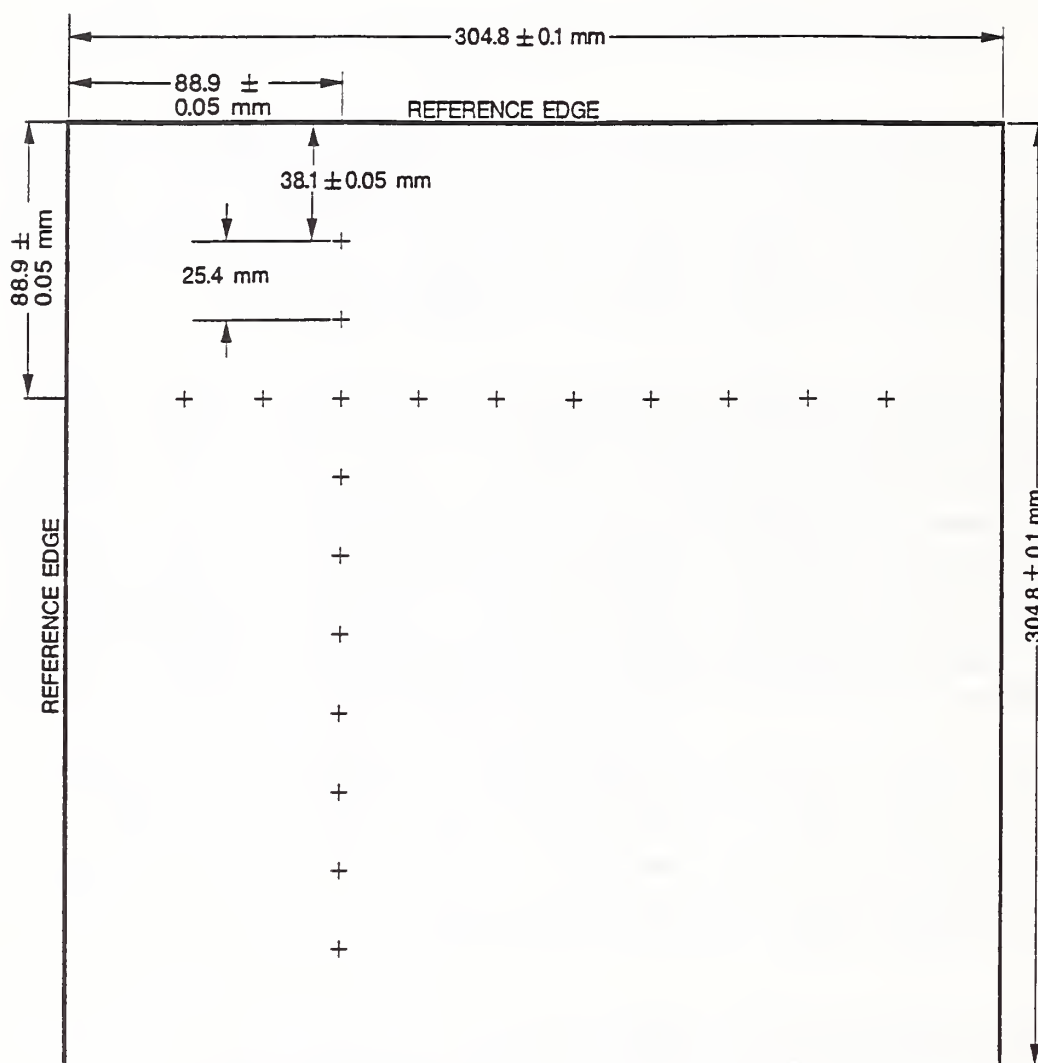
Our approach has been to learn of standardization needs from radioscopy systems users through participation in American Society for Testing and Materials (ASTM) Subcommittee E07.01 on Radiology and through discussions with system users groups. For example, users of laminography systems (a special subset of automated radioscopy that can focus on a single plane) for circuit board inspection identified a need for several calibration devices [1]. In a joint program with the U.S. Army Harry Diamond Laboratory, we satisfied one of these needs by developing a calibration board for the X-Y stages of automated radioscopy systems. The board, shown in Figure 1, was designed to directly measure the positioning accuracy and geometrical magnification of the system by the use of calibrated holes. The first stocking order of this standard material (SRM 1842) was produced and verified. It is available for purchase from the NIST Office of Standard Reference Materials in Gaithersburg, (301) 975-6776.

The cooperative radioscopy standards development program with the Harry Diamond Laboratory is continuing. This next year we will complete the development of a second standard material, one to measure the depth of focus and the Z-dimension resolution of laminography systems. This device is a series of alternate layers of high- and low-density material. As the plane of focus is moved up or down, the high-density layers move in and out of focus. Optical calibration of the layer positions (furnished with the device) allows users to calibrate the Z-dimension of their system.

In test method development, we have been working closely with ASTM Subcommittee E07.01 on Nondestructive Testing. This committee contains representatives of the industrial developers and users of this technology, and is responsible for maintaining a wide variety of x-ray testing procedures and standards. We have been assisting in the preparation of new standards for radioscopy that parallel the older standards for film-based radiography. We just drafted a proposed standard for the use of British Standard 3971 duplex wire gages for use with radiologic imaging applications. This document will be balloted by the ASTM Subcommittee E07.01 in the next few months.

NIST has also been working with the General Electric Company, the Naval Air Engineering Center, and the U.S. Army Materials Technology Laboratory in developing an ASTM standard for radioscopic inspection of military components. In accordance with a Department of Defense desire to avoid the preparation of separate military standards, the standard will be a supplement to a general ASTM standard (E1255) on radioscopic inspection. The sixth draft of this standard completed balloting within ASTM Committee E07 and was also through the Department of Defense laboratory review. It should be published within the next year.

X-RAY LAMINOGRAPHY CALIBRATION PLATE

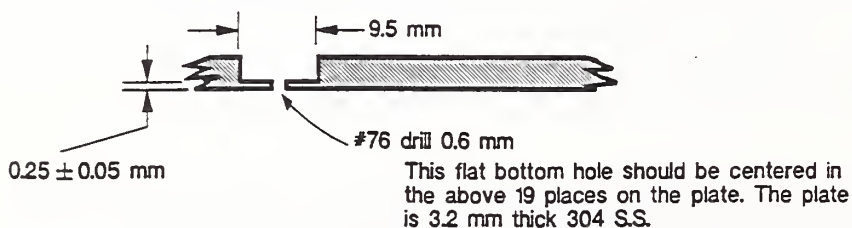**Fig. 1.** Calibration board for confirming the X-Y stage positioning accuracy and magnification of an automated x-ray radioscopy system.

In several cases, we developed new ideas for standards but were not been able to contact users with an immediate need within ASTM Committee E07 or organized users groups. In these cases, we published reports of the concepts and invited participation in round robin evaluations. One concept was

a hollow sphere design that seems to be particularly useful for systems that permit rotation of the parts being inspected [2]. Another was a twisted strip image quality indicator design for characterizing a microfocus x-ray tube beam [3]. Here, the concept is simply that of a thin strip with a half twist. The twist allows the large dimension of the strip cross section to be perfectly oriented with the x-ray beam at some location, without careful orientation of the strip itself. We provided samples of both concepts to potential users and are awaiting reports of their evaluations.

The rest of the world is also quite interested in implementing radioscopic inspection technology. The International Institute of Welding Commission V is developing a number of standards for this technique, which they will submit to the International Standards Organization as draft standards. NIST is serving as liaison between ASTM and IIW, so U.S. standards will be compatible with the rest of the world. During this next year, we will supply one of our X-Y stage calibration board for consideration as an international standard (ISO). To make American industry aware of these international activities, we have published summaries of the annual meetings for the NDE community [4-6].

REFERENCES

1.   T. A. Siewert, M. W. Austin, G. K. Lucey, and M. J. Plott, "Evaluation and Qualification Standards for an X-ray Laminography System," Materials Evaluation, **50**, 1027 (1992).

2.   T. A. Siewert, D. W. Fitting, and M. W. Austin, "Rotationally Symmetric Image Quality Indicator for Digital Imaging Systems," Materials Evaluation, **50**, 360 (1992).

3.   T. A. Siewert and M. W. Austin, "An X-ray Image Quality Indicator Designed for Easy Alignment," Materials Evaluation, **50**, 1069, (1992), also distributed as International Institute of Welding Document V-965-91, available from the American Council of the IIW, American Welding Society, Miami, Florida, 1991.

4.   T. A. Siewert, "Report on 1990 Actions by the International Institute of Welding," Materials Evaluation, **49**, 470 (1991).

5.   T. A. Siewert, "Report on 1991 Actions by International Institute of Welding," Materials Evaluation, **50**, 422 (1992).

6.   T. A. Siewert, "Report on 1992 Actions by International Institute of Welding," submitted to Materials Evaluation.

Acoustic Emission and Ultrasonic Methods and Standards

G. V. Blessing (301-975-6627)
Automated Production Technology Division, Manufacturing Engineering Laboratory

The objective of this program is to acquire a better understanding of acoustic emission sensors, ultrasonic sensors and reference artifacts for application to improved standards for industry. This purview includes the sensitivity of acoustic emission sensors to material surface displacements as a function of rise time. Another area of interest is the beam profile and energy output of an ultrasonic sensor acting as a source, and its sensitivity dependence on frequency as a receiver. Also included is the design of reference artifact targets to study the sensor and entire ultrasonic system response to target echoes.

Last year's effort focused on expanding the application of transmitter/receiver sensors, used in pulse-echo calibrations, to a wider range of flat-bottom-hole (f-b-h) reference artifact target dimensions. Background to this work is the ASTM E127 document titled "Standard Practice for Fabricating and Checking Aluminum Alloy Ultrasonic Standard Reference Blocks," a practice that has undergone few changes since its original promulgation 35 years ago. The basic approach to the standard is to fabricate f-b-h (cylindrical) aluminum blocks of known material quality to precise geometrical standards, such that the pulse-echo response values from the f-b-h targets of specific diameters and depths meet certain acceptance criteria. Due in large part to its requirement that 5 MHz quartz transducers be used in the measurement of the block response values, this standard has become too restrictive for industry's present needs. Specifically, the quartz sensor limits the range of block sizes (i.e., metal distances between wave entry surface and the hole bottom) and hole sizes that can be reliably measured.

Quartz transducers are intrinsically narrowband devices with a low electro-acoustic and acousto-electric transduction efficiency compared to ceramic transducers which are widely used by the ultrasonic industry. Because of their narrowband characteristics there results a limited near-surface resolution which prevents application to blocks shorter than a 13 mm metal distance. Their limited sensitivity inhibits application to blocks with longer than a 150 mm metal distance. This low sensitivity also inhibits the inspection of smaller than 1.2 mm f-b-h diameters in the longer metal-path blocks, a growing requirement in the industry. Furthermore, quartz sensors fabricated to the standard's specifications are expensive, not readily available, and require unconventional tuned pulsers to drive them. Consequently, industry now has a strong desire to substitute ceramic sensors for quartz sensors in the E127 practice.

This past year an interlaboratory effort involving industry and NIST was begun to (1) evaluate the use of ceramic sensors at a higher frequency (10 MHz) for shorter (down to 1.5 mm metal distance) blocks with the 1.2, 2.0 and 3.2 mm f-b-h diameters of the present E127 standard. Two additional aspects of this effort were to (2) test for a simplified and improved-precision procedure to make gain changes in the E127 standard, and to (3) retain the same acceptance criteria for the f-b-h response values as had been established in the application of quartz sensors to blocks in the 13 to 150 mm metal-distance range. Industry laboratories with a significant interest in this effort include Reynolds Metals, ALCOA, Kaiser Aluminum, Harisonics (Staveley Instruments), and Panametrics. The following are some initial conclusions from this collaboration.

(1) Each participating laboratory evaluated its own broadband pulser/receiver system for linearity, and its own 10 MHz ceramic sensor(s) 13 mm in diameter for beam profile and spectral content. For a near-surface resolution of 1.5 mm on the shortest metal-path block, the echo pulse width must be less than 0.5 μs, i.e. the time difference between the front surface and f-b-h echoes. The several commercially available and commonly used systems evaluated were minimally capable of this resolution in conjunction with the ceramic sensors.

(2) When calibrating different f-b-h diameter blocks for their echo response, gain changes proportional to their relative diameters are necessary in order to apply a common accept/reject criteria to all blocks for their echo-amplitude response values. A general consensus was reached to consider making receiver gain changes based on the ratio of f-b-h areas, and to eventually replace the traditional E127 procedure which uses secondary-reference steel ball targets. This would be a less cumbersome procedure yielding more precise results.

(3) The last part of this effort was to evaluate whether the acceptance criteria, established in E127 for a quartz-sensor system, would apply to a ceramic-sensor system when adjusting the system gain such that the response value from one particular block (13 mm metal path) matched that using E127 procedures. This proved futile, and can be understood in light of the significant far-field-beam profile differences that exist between sensors of differing aperture and spectral content (5 MHz quartz and 10 MHz ceramic in this instance). Echo amplitude response differences of 2 to 4 dB between the two systems were typically observed for a given block. This is in contrast with a nominal goal of a 1 dB difference.

Several possibilities for future direction may be considered. One is the design and fabrication of ceramic sensors with the same frequency and comparable dimensions to the quartz sensors, such that their far-field profiles are matched. This does not resolve the problem, however, of inspecting short metal-distance blocks which intrinsically requires higher-frequency sensors. Another fundamentally different approach is to make block-to-block comparisons. This is a rather robust approach wherein arbitrary sensors and systems are used to compare new (uncalibrated) blocks with "accepted" blocks. The industry user thereby generates a correction factor for each new block, securing it to a known reference block. Promising results have been obtained with both ceramic and quartz 5 MHz sensors using this approach on a limited range of block sizes.

Thermal and Electrical Properties of Copper-Tin and Nickel-Tin Intermetallics

H. P. R. Frederikse[2] (301-942-0754), and A. Feldman (301-975-5740)
Ceramics Division, Materials Science and Engineering Laboratory

R. J. Fields
Metallurgy Division, Materials Science and Engineering Laboratory

The OIPM 1991 Annual Report contains a detailed description of several research projects related to processing and inspection of soldered joints for electronic components. Attention was focused on two intermetallic compounds, Cu_6Sn_5 and Cu_3Sn, which are formed in solder joints at the Cu-(Pb/Sn) interface. The 1991 report deals with the phases, morphology and mechanical properties of the Cu-Sn compounds.

During FY 1991 and the beginning of FY 1992, a parallel research effort was aimed at the investigation of several physical properties of Cu-Sn (and Ni-Sn) intermetallics, in particular, the thermal diffusivity (or thermal conductivity), the electrical resistivity, the heat capacity and the density. The technique used to determine the thermal diffusivity was photothermal radiometry (PTR). The heat capacity was measured by means of differential scanning calorimetry (DSC). Two techniques were employed to measure the electrical resistivity of the intermetallics: the eddy current method and the van der Pauw method. The density was derived from accurate determinations of the weight and of the dimensions of precision ground cylinders of the compounds.

The following results were obtained: (1) The simultaneous measurements of the thermal conductivity κ (deduced from the thermal diffusivity) and the electrical conductivity σ, made it possible to test the validity of the Wiedemann-Franz law relating these two quantities: $\kappa/\sigma = LT$ (where T is the absolute temperature and L the Lorentz number). The agreement with the theoretical predictions/appeared to be satisfactory. (2) The thermal and electrical conductivity of these intermetallics are of the same order of those of Pb/Sn solder. (3) Compared with copper the thermal conductivity is about 6 to 20 times smaller; electrical conductivity is 1/5 to 1/15 of the value for copper.

PUBLICATION

1.   H. P. R. Frederikse, R. J. Fields, and A. Feldman, "Thermal and Electrical Properties of Copper-Tin and Nickel-Tin Intermetallics," J. Appl. Phys. 72, 2879 (1992).

---

[2] Consultant to Ceramics Division, Materials Science and Engineering Laboratory

PERSONNEL

The permanent staff of the Office of Intelligent Processing of Materials is listed below.

OIPM PERMANENT STAFF IN FISCAL YEAR 1992

H. Thomas Yolken, Chief   Patty Salpino, Administrative Officer
Vacant, Deputy Chief*   Ellen Altman, Secretary
George Birnbaum, Senior Scientist* Linda Souders, Secretary

*In the absence of a Deputy Chief, Dr. Fred Mopsik of the Polymers Division served as a part-time staff member from September 1, 1992 to February 24, 1992. Since February 24, 1992, Dr. George Birnbaum has assumed some of the duties of the Deputy Chief.

A. OIPM SEMINARS AT NIST

Ray T. Ko, Ohio State University, Columbus, Ohio, "Ultrasonic Evaluation of Interfacial Properties in a Layered Substrate," September 16, 1992.

Professor W. K. Arnold, Fraunhofer-Institute for Non-Destructive Testing, Federal Republic of Germany, "Generation and Detection of Ultrasound by Lasers and its Applications," June 18, 1992.

Dr. Kumar Wickramasinghe, T. J. Watson Research Center, Yorktown, NY, "Nanometer Microscopy of Physical Properties," May 14, 1992.

Claudio Pecorari, Ohio State University, Columbus, Ohio, "Investigation of Ultrasonic Plane Wave Scattering by a Randomly Rough Solid-Solid Interface," November 4, 1991.

Professor Alan C. F. Cocks, Cambridge University Engineering Department, Cambridge, England, "Modeling of Diffusional Mechanisms of Creep and Sintering," Joint IPM/Metallurgy Seminar, September 24, 1992.

B. INVITED TALKS AND PAPERS BY OIPM STAFF

"Consortium on Intelligent Processing of Rapidly Solidified Metal Powders," H. T. Yolken, NIST Visiting Committee, Boulder, Colorado, June 9, 1992.

"Intelligent Processing of Materials," H. T. Yolken, National Research Council Study Group, Woods Hole, Mass., August 19, 1992.

"The Role of Process Models in Processing of Materials," H. T. Yolken, ASM Heat Treatment Steering Panel, Chicago, Ill., September 21, 1992.

"Research in NDE Sensors for Materials Processing at the National Institute of Standards and Technology," G. Birnbaum, Penn State's Nondestructive Test and Evaluation Showcase, Pennsylvania

State University, PA, October 15, 1991.

"The Contributions of Ternary Collisions to Collision-Induced Line Shapes," G. Birnbaum, Department of Physics, University of Guelph, Guelph, Canada, November 30, 1991.

"Intelligent Processing of Materials," G. Birnbaum, Office of Science and Technology Policy, Committee on Materials, Working Group on NDI/E, Institute for Defense Analysis, Alexandria, VA, July 7, 1992.

"Molecular Interactions and the Shape of Pressure Broadened Infrared Lines," G. Birnbaum, Chemistry Department Seminar, University of Nevada, Reno, Nevada, January 27, 1992.

"Recent Developments in NDE Measurements and Standards in NIST," G. Birnbaum, D. G. Eitzen, and L. Mordfin, in Nondestructive Testing Standards - Present and Future - ASTM STP 1151, H. Berger and L. Mordfin, Eds., American Association for Testing Materials, Philadelphia, PA, 1992, pp. 89-125.

C. SPONSORED WORKSHOPS

Polymer Blends Consortium, Industrial Workshop to Plan a Consortium on Intelligent Processing of Polymer Blends, April 20-21, 1992.

Polymer Processing Consortium, Industrial Workshop to Plan a Consortium on Sensing for Polymer Processing, March 16, 1992.

Coating Technology Consortium, Industrial Workshop to Plan a Consortium on Coatings Technology, February 19-20, 1992, and June 23, 1992.

Ceramic Processing Consortium, Industrial Workshop to Plan a Consortium on Intelligent Processing Ceramic Slurries, June 15-16, 1992.

Casting of Aerospace Alloys, Industrial Workshop to Plan a Consortium on Casting of Aerospace Alloys, January 16, 1992, and April 28, 1992.

D. COMMITTEES, CONFERENCES, AND OTHER INVITED PARTICIPATION BY OIPM STAFF

H. Thomas Yolken

Board of Directors, American Society for Nondestructive Evaluation
Editor-in-Chief, Research in Nondestructive Evaluation
ASM - Heat Treatment Steering Panel
Review Panel (NSF) for MIT Manufacturing Center
Evaluation Panel, Lawrence Livermore Labs NDE Program
Principle Co-chairman for First ASNT Research Symposium on NDE
Steering Committee, Sixth International Meeting on Materials Characterization

G. Birnbaum

Editorial Board, Research in Nondestructive Evaluation
Associate Editor, Journal of Quantitative Spectroscopy and Radiative Transfer
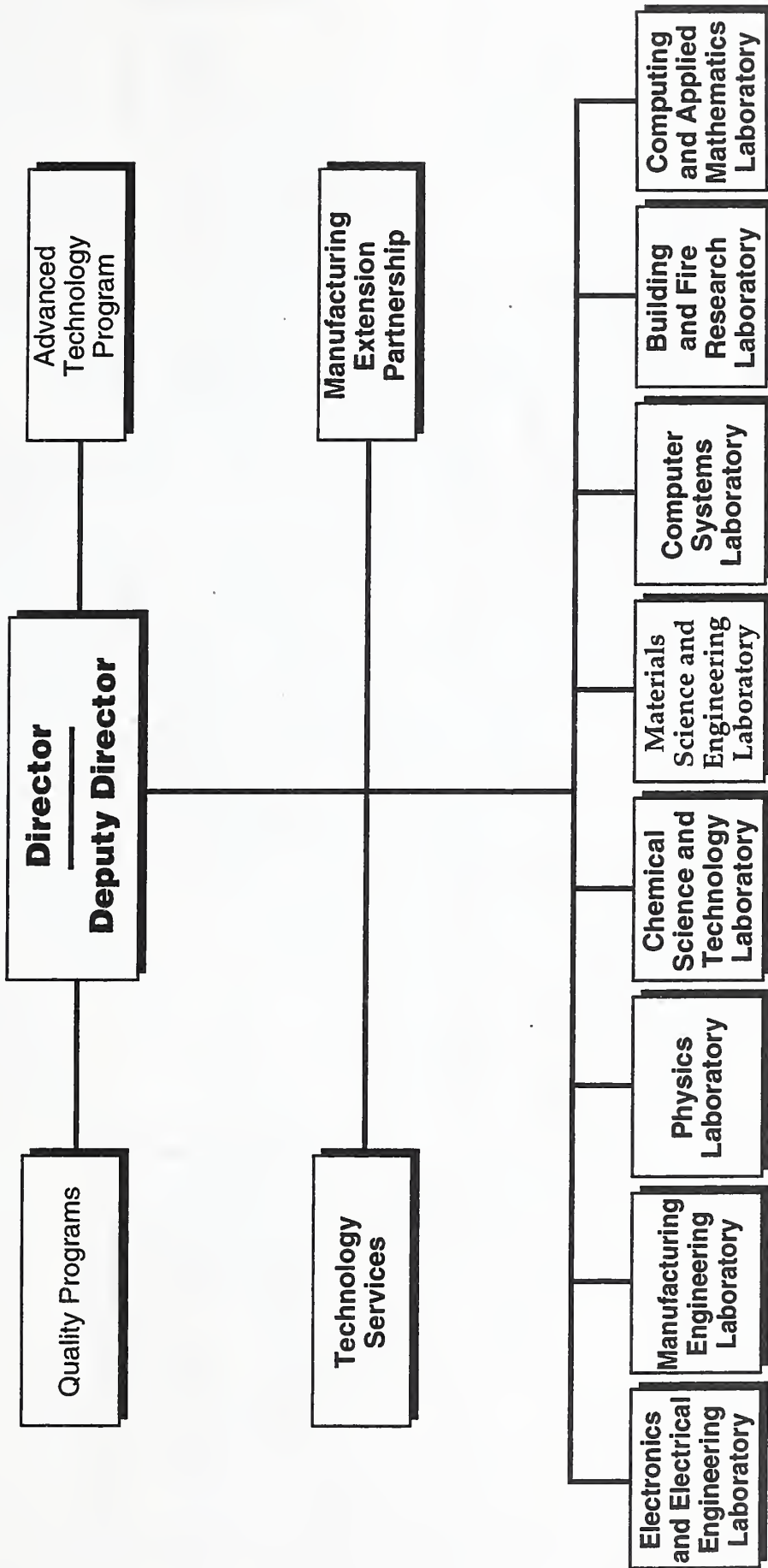
MATERIALS SCIENCE AND ENGINEERING LABORATORY

L.H. Schwartz, Director
H.L. Rook, Deputy Director

Institute Scientists

J.W. Cahn
R.M. Thomson
S.M. Wiederhorn
B.R. Lawn

Intelligent Processing of Materials

H.T. Yolken, Chief

Ceramics

S.W. Freiman, Chief
S.J. Dapkunas, Deputy

Reactor Radiation

J.M. Rowe, Chief
T.M. Raby, Deputy

Polymers

L.E. Smith Chief
B.M. Fanconi, Deputy

Metallurgy

E.N. Pugh, Chief
S.C. Hardy, Deputy

Materials Reliability

H.I. McHenry, Chief
C.M. Fortunko, Deputy